TECHNISCHE UNIVERSITÄT MÜNCHEN

Fakultät für Medizin

Clinical relevance of kallikrein-related peptidases in advanced high-grade serous ovarian (KLK11, KLK15) and in triple-negative breast cancer (KLK11)

Xiaocong Geng

Vollständiger Abdruck der von der Fakultät für Medizin

der Technischen Universität München zur Erlangung des akademischen Grades eines

Doktors der Medizin (Dr. med.)

genehmigten Dissertation.

Vorsitzender: Prof. Dr. Jürgen Schlegel

Prüfer der Dissertation:

1. apl. Prof. Dr. Viktor Magdolen

2. apl. Prof. Dr. Birgit Luber

Die Dissertation wurde am 05.03.2019 bei der Technischen

Universität München eingereicht und durch die Fakultät für Medizin

am 13.08.2019 angenommen.

When I have fears that I may cease to be

Before my pen has glean'd my teeming brain,

Before high piled books, in charact'ry,

Hold like rich garners the full-ripen'd grain;

When I behold, upon the night's starr'd face,

Huge cloudy symbols of a high romance,

And think that I may never live to trace

Their shadows, with the magic hand of chance;

And when I feel, fair creature of an hour!

That I shall never look upon thee more,

Never have relish in the faery power

Of unreflecting love!—then on the shore

Of the wide world I stand alone, and think

Till Love and Fame to nothingness do sink.

–John Keats, 1848

Contents

List of Tables

List of figures

1. Introduction

1.1 Ovarian cancer

1.1.1 Epidemiology

Ovarian cancer is one of the most common gynecological malignancies in women. Each year, about 200,000 women develop ovarian cancer worldwide with an estimated five year survival rate of about 45% (Torre et al., 2018). The high mortality rate is due to late stage diagnosis because of the absence of early symptoms and high recurrence rates despite aggressive primary therapy (Jayson et al., 2014). The attempt of screening the population for serum cancer antigen 125 (CA125) combined with transvaginal ultrasound (TVUS) proved to be insufficient concerning detecting curable cancer at early stages (Buys et al., 2011). Clinical symptoms of ovarian cancer typically represent abdominal pain or distension for months (Goff et al., 2004), which might be incorrectly attributed to gastrointestinal disorders. Protective factors for ovarian cancer usually involve pregnancy, breast feeding, and/or the use of oral contraceptives (Wentzensen et al., 2016). Increased risk for the development of ovarian cancer has been linked to family history, genetic predisposition, e.g. mutations in BRCA1/2 genes (Jayson et al., 2014; King et al., 2003), and benign ovarian disorders, such as endometriosis and polycystic ovaries (Wiegand et al., 2010).

1.1.2 Histological classification

The histological classification of ovarian cancer has evolved from an epithelial-derived tumor to distinct subtypes. Approximately 90% of all ovary cancers are epithelial, whereas non-epithelial types include sex cord-stromal, germ cell, and indeterminate tumors (Holschneider et al., 2000). In epithelial phenotypes, about 10-20% of cases are borderline or low malignant tumors. In invasive epithelial subpopulations, over 70% of cases belong to serous carcinomas, while others include mucinous, endometrioid, clear

cell, transitional (Brenner), small cell, and undifferentiated carcinomas (Holschneider et al., 2000). Generally, ovarian cancer is proposed to be classified into two types (Cho and Shih, 2009). The type I group comprises low-grade serous, low-grade endometrioid, mucinous, clear cell, and Brenner tumors. These tumors are confined to the ovary at the time of diagnosis and are less aggressive. The type I carcinomas display a pathology generation pattern from the intermediate steps (so-called borderline tumors) supporting a morphologic lineage progression of these ovarian carcinomas. The type II group tumors are composed of high-grade serous, high-grade endometrioid, malignant mixed mesodermal, and undifferentiated carcinomas. They are highly aggressive, usually showing advanced stages at the time of diagnosis. The morphologic differences between type I and type II tumors are also due to differences in somatic mutations. In the type I group, KRAS, BRAF, and ERBB2 mutations occur in approximately two thirds of the low-grade serous subtype, whereas TP53 mutations are rare in those tumors. In contrast, in the type II group, TP53 mutations are displayed in over 80% of the cases. Moreover, type II tumors rarely harbor mutations that are typical for type I tumors (Kurman et al., 2010) (**Figure 1**).

Concerning pathogenesis of ovarian cancer, it was previously speculated that epithelial ovarian cells are the origin of high-grade serous ovarian cancers (HGSOCs). However, recent studies have proposed that the fallopian tube quite likely represents the progenitor of a substantial proportion of HGSOCs rather than developing *de novo* from the ovary. This is due to the fact that precursor lesions found in the fimbriae of the fallopian tube resemble HGSOCs in both morphological and molecular aspects (Karnezis et al., 2017; Soong et al., 2018). Moreover, in the studies using preventive salpingo-oophorectomy for reducing family predisposition of ovarian tumors, a high prevalence of tubal-arising carcinoma in the resected tissue was found (Howitt et al., 2015; Perets et al., 2013). In those HGSOCs arising without apparent fallopian tube involvement, a possible mechanism suggests that the normal tubal epithelium from the fimbria implants on the site of rupture following ovulation and then undergoes malignant transformation. The propensity of HGSOCs for omental metastasis support

this mechanism, because the fallopian tube arising of ovarian tumors could roughly overcome the abdomen spread barrier without vasculature assistance (Pradeep et al., 2014).

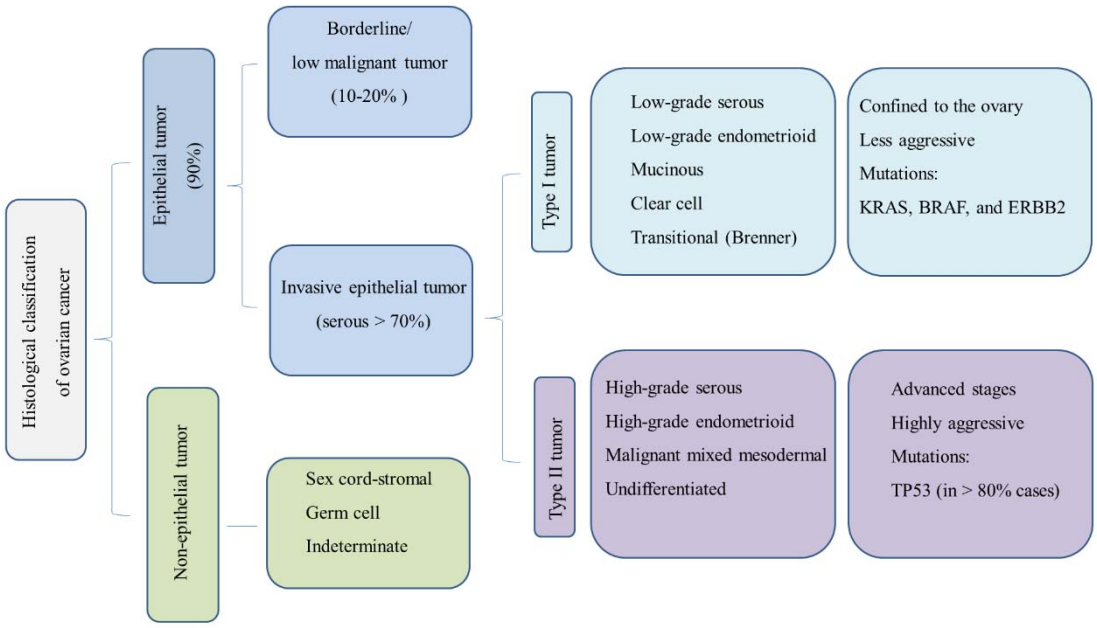

Figure 1. **Histological subgroups of ovarian cancer.**
Ovarian cancer is divided into epithelial (90%) and non-epithelial types (sex cord-stromal, germ cell, and indeterminate tumors). The epithelial types are further subdivided into borderline/low malignant tumors (10-20%) and invasive subtypes (serous, mucinous, endometrioid, clear cell, transitional (Brenner), small cell, and undifferentiated tumors. Invasive ovarian cancer is then classified into the type I group (low-grade serous, low-grade endometrioid, mucinous, clear cell, and Brenner tumors) and the type II group (high-grade serous, high-grade endometrioid, malignant mixed mesodermal, and undifferentiated carcinomas).

1.1.3 Therapy of ovarian cancer

To date, primary debulking surgery, including hysterectomy, bilateral salpingo-oophorectomy, infragastric omentectomy, and - if indicated - pelvic and paraaortal lymph node dissection with the goal of removal of all visible tumor tissue is standard of care (Jayson et al., 2014). The clinical staging of ovarian cancer (FIGO stage, **Appendix 7.1**) is based on the comprehensive surgery. After the tumor debulking

surgery, platinum-based chemotherapy is administered. Carboplatin is combined with paclitaxel and the angiogenesis inhibitor bevacizumab (via inhibition of VEGF-A) in advanced stages. However, advanced ovarian tumors often develop platinum resistance thus allowing recurrence. Therefore, it is a challenge to search for new and effective chemotherapeutic drugs.

1.1.4 High-grade serous ovarian cancer (HGSOC)

High-grade serous ovarian carcinomas account for the majority of ovarian cancer cases. HGSOC is characterized by an advanced stage at diagnosis and an aggressive behavior during tumor progression. Therefore, the five year survival rate of HGSOC is only 35-40% (Bowtell et al., 2015). The genetic profile of HGSOC, which has been validated via large-scale genomic studies (Ciriello et al., 2013), convincingly supports the separation of HGSOCs from the other ovarian cancer subgroups (Bell et al., 2011). In over 80% of HGSOCs, deleting mutations in the TP53 gene occur (Kurman et al., 2010; Kuhn et al., 2012). Approximately half of HGSOC patients harbor mutations in BRCA1/2 and/or other genes involved in the homologous recombination (HR) pathway (Bell et al., 2011; Strickland et al., 2016). In those HGSOC patients, who show no apparent defects in HR, disordered amplification of the CCNE1 gene encoding cyclin E1 occurs in approximately 30% (Bell et al., 2011; Au-Yeung et al., 2017). An increased number of aberrations of the MYC gene was documented in over 80% of HGSOC cases (Bell et al., 2011; Xu et al., 2017). Other tumor-relevant genes, frequently mutated in HGSOC patients, include RB, PI3K, NOTCH, and FOXM1 (Tothill et al., 2008).

Although HGSOCs excellently respond to routine platinum-based chemotherapy, development of drug resistance combined with a relapse often occurs within six to twelve months after primary treatment. Advancement beyond current standard chemotherapy turns out to be difficult. Inhibitors of poly ADP-ribose polymerase (PARP) have been administered in patients who suffered from recurrent disease following platinum-chemotherapy irrespective of the BRCA status (Ledermann and El-

Khouly, 2015). For example, olaparib plus chemotherapy followed by maintenance therapy significantly improved progression-free survival (Pujade-Lauraine et al., 2017; Gelmon et al., 2011). Niraparib significantly improved PFS regardless of the presence BRCA mutations (Mirza et al., 2016). The use of the PARP inhibitor rucaparib in the adjuvant setting and/or in combination with anti-angiogenic drugs is now the subject of clinical trials (Sabatucci et al., 2018).

1.2 Breast cancer

1.2.1 Epidemiology

Breast cancer is one of the three most common malignancies worldwide, and the most common one in women (DeSantis et al., 2014). One out of eight to ten women will probably suffer from breast cancer throughout their lifetime (Harbeck and Gnant, 2015). A study from the National Cancer Institute in the US reported an increased incidence of breast cancer (both ductal carcinoma *in situ* [DCIS] and invasive subtypes) worldwide since the 1970s (Noone et al., 2018). Nevertheless, in developed countries, a decreased mortality is emerging, due to early detection by widespread mammography screening and efficient systemic treatment. For example, the mortality of breast cancer in Europe dropped by 8% in 2016 (Malvezzi et al., 2016). However, in less developed countries, the mortality of breast cancer is still increasing, constituting the majority of cancerous deaths in women (Torre et al., 2012). In over 80% of the cases, the primary symptoms of breast cancer are distinct nodes in the mammary tissue. About 20% of the nodes detected in the armpit and located in lymph nodes turn out to be afflicted with breast cancer. Other symptoms include size changes of one breast, alterations in shape or position of nipples, discharge from nipples, skin puckering or dimpling, and chronic pain in breasts or armpits. Primary risk factors of breast cancer encompass a positive family history of breast cancer, high estrogen levels, no/late giving birth, obesity, and postmenopausal hormone replacement therapy (Carlson et al., 2009). In addition, about 5-10% of breast cancers could be connected to germline mutations in BRCA1 and/or

BRCA2 genes (King et al., 2003). In these women, the lifetime risk for the development of breast cancer is 40-85% (Kuchenbaecker et al., 2017).

1.2.2 Histological classification

Breast cancer diagnosis implies breast imaging via mammography with subsequent verification by core biopsy. Subtype determination by immunohistochemistry contributes profoundly to the choice of a clinical treatment option. For all tumor specimens, hematoxylin and eosin (H&E) staining together with immunohistochemical analyses, reveals the expression profiles of three important receptors in cancer cells, namely of the estrogen receptor (ER), of the progesterone receptor (PR), and of the human epidermal growth factor receptor 2 (HER2), as well as grading and the proliferation rate (Ki-67). The efforts to identify genome-wide molecular features of breast tumors were accomplished by Perou and co-workers in 2000 (Perou et al., 2000). Since then, many studies have reported associations between progression of breast cancer with its molecular subtypes, as well as the morphological ones. Breast cancer is usually categorized by its histological origin which are from the inner lining epithelium of either the duct (ductal carcinoma) or the lobule (lobular carcinoma). The morphological subgroups are also based on the criterium whether the carcinoma is limited to the epithelium (*in situ* carcinoma) or has invaded to the stroma and/or other tissue (invasive carcinoma). Concerning carcinomas *in situ*, the ductal carcinoma *in situ* (DCIS) is more common than the lobular carcinoma *in situ* (LCIS) including five well recognized subtypes (comedo, cribiform, micropapillary, papillary, and solid tumors). The major invasive tumor types include infltrating ductal, invasive lobular, ductal/lobular, mucinous (colloid), tubular, medullary, and papillary carcinomas (Malhotra et al., 2010). Nowadays, distinct subtypes based on gene expression profiles have been generally accepted and are utilized in the clinic, including luminal A, luminal B, HER2 positive, and triple-negative subtypes (Harbeck and Gnant, 2017). Luminal A accounts for about 40% of invasive breast cancers. It is ER and/or PR positive, HER2 negative or low,

and shows low proliferation (Ki-67). Luminal B comprises about 20% of invasive breast cancers. Here, the ER and/or PR is positive, while HER2/neu is variable positive or negative, and the proliferation rate (Ki-67) is higher than in luminal A. The HER2 positive group accounts for 10-15% of invasive breast cancers with ER and PR usually being negative and HER2/neu strongly positive. This group of breast cancer shows poor prognosis and responds to trastuzumab therapy. The triple-negative class comprises about 15-20% of invasive breast cancers, with ER and PR negative, and HER2 negative/low (triple negative). High proliferation rate and TP53 mutations are common in this type. Other molecular subtypes of breast cancer have been suggested by studies including normal-like breast cancer displaying normal adipose tissue gene signatures and basal-like breast cancer with high frenquency of CK5/6 and EGFR mutations (Makki, 2015; Malhotra et al., 2010) (**Figure 2**).

1.2.3 Therapy of breast cancer

Traditional therapies of breast carcinomas include tumor resection and radiotherapy (Gradishar et al., 2015). Nowadays, the conventional surgery to achieve complete tumor resection might no longer be the standard therapy for all patients. Systemic therapy standards have been established in clinical practice for selected tumors, which combine other therapeutic options encompassing chemotherapy, endocrine therapy, and targeted therapy, administered adjuvantly or neoadjuvantly. For example, the monoclonal antibodies (trastuzumab and pertuzumab) have been used for HER2+ breast cancer patients. The estrogen-receptor antagonist tamoxifen has been used for ER+ patients (Curigliano et al., 2017). If chemotherapy is indicated, it is recommended to administer a neoadjuvant regimen in triple-negative and HER2+ phenotypes (Denkert et al., 2017).

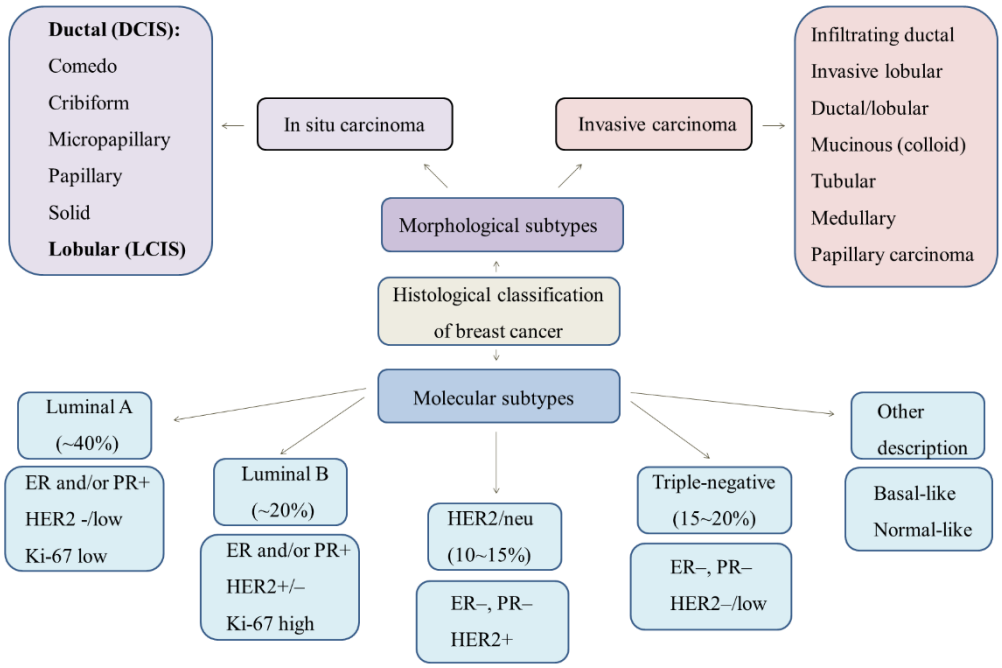

Figure 2. Histological classification of breast cancer.

Breast cancer is usually categorized by its histological arising into the ductal or the lobular carcinoma. The morphological subgroups are also divided into *in situ* and invasive carcinoma. The ductal carcinoma *in situ* (DCIS) is more common than the lobular carcinoma *in situ* (LCIS), which includes five subtypes (comedo, cribiform, micropapillary, papillary and solid tumors). The major invasive tumor types include infltrating ductal, invasive lobular, ductal/lobular, mucinous (colloid), tubular, medullary and papillary carcinomas. Molecular categorization of invasive breast cancer has five major subtypes. Luminal A accounts for about 40% cases. It is ER and/or PR positive, HER2 negative or low, and displays low proliferation (Ki-67). Luminal B comprises about 20% cases with ER and/or PR positive, while HER2/neu is variably positive or negative, and the proliferation rate (Ki-67) is higher than in luminal A. The HER2 positive group accounts for 10-15% cases. Here, the ER and PR are usually negative, ER2/neu is strongly positive. The triple-negative class comprises about 15-20% of invasive breast cancers, with ER and PR negative and HER2 negative/low (triple-negative).

1.2.4. Triple-negative breast cancer

Triple-negative breast cancer (TNBC) refers to a molecular profile lacking all three clinical relevant receptors: the estrogen receptor, the progesterone receptor, and the Her2/neu (HER2) receptor (Foulkes et al., 2010; Patch et al., 2015). Basal-like breast cancer (BLBC) is similar to TNBC because BLBC cells are often characterized by the absence of receptors for estrogen, progesterone and HER2. However, in BLBC cells expression of selected proteins may differ from that of TNBC cells (Perou et al., 2000; Anderson et al., 2014). Therefore, not all BLBCs are TNBCs and *vice versa*. TNBCs account for approximately 15-20% of all breast cancers. Patients suffering from TNBC are more often observed in younger women (<50 years) and in the ethnic African-American group (Elsawaf et al., 2011). Invasive ductal carcinomas are among the most frequent cases of TNBC, followed by various tumor subtypes including metaplastic, medullary, apocrine, adenoid cystic lesions, and invasive lobular carcinomas (Ishikawa et al., 2011; Lehmann et al., 2011). Germline mutations that are linked to the development of TNBC remain elusive. Similar to other subtypes of breast cancer, patients suffering from TNBC consistently show clinico-pathological indicators such as BRCA1 dysfunction (Ibrahim et al., 2012). Mutations in the p53 gene were reported to be associated with an unstable subtype of TNBC, accompanied by activation of the downstream phosphatidylinositol-3 kinase pathway (Costa et al., 2018). Additional mutations described in TNBCs and BLBCs include the myelocytomatosis oncogene, the kinase insert domain receptor, CK5/6, EGFR1, caveolin 1/2, cyclin-D1 and P-cadherin (Dillon et al., 2016; Ossovskaya et al., 2011).

Because TNBC is highly aggressive, the diagnosis of TNBC indicates adverse clinico-pathological signatures of tumor tissue (e.g. unfavorable molecular markers, rapid tumor cell proliferation, and high histological grade), and poor long-time prognosis of patients (e.g. frequent invasion via vasculature and lymphatic vessel, high tendency of relapse and early distant metastasis) (Foulkes et al., 2010; Lehmann et al., 2016). TNBC patients very often relapse, whereby a distant recurrence is highly probable within three

years, followed by death within five years after primary diagnosis. After this time window, the sharply declined risk seems to turn to a risk comparable to other breast tumors (Foulkes et al., 2010).

Standard therapy for TNBC involves neoadjuvant chemotherapy including anthracyclines, taxanes and carboplatin followed by surgery with/without radiotherapy (Harbeck and Gnant, 2017). Due to the deficiency in expression of ER, PR, and HER2, these targets addressed in receptor-positive subtypes of breast cancer, cannot be used in treatment of TNBC (Hu et al., 2017). Nevertheless, TNBCs as well as BLBCs, have preserved the susceptibiliy for a complete response to adjuvant and/or neo-adjuvant chemotherapies, including administration of taxanes, anthracyclines, and cyclophosphamide (Perez et al., 2010). However, though TNBC patients respond to chemotherapy, it cannot guarantee a favorable prognosis in all cases. Therefore, new pharmacological targets have been investigated in numerous studies and clinical trials in terms of improvement of survival of TNBC patients. PARP inhibitors were proposed to improve survival outcome in patients afflicted with BRCA1/2 mutations (Rottenberg et al., 2008; Geenen et al., 2018). In cases of PI3K/AKT/mTOR activation, the therapeutic potential of rapamycin inhibitors was successfully tested (Mo et al., 2016). Since the growth pattern of TNBCs involves lymphocyte infiltration, checkpoint programmed death 1 and programmed death-ligand 1 (PD-1 and PD-L1) inhibitors were incorporated in clinical trials as promising candidates (Salgado et al., 2015; Hida et al., 2016). Moreover, anti-angiogenic agents (e.g. bevacizumab and sunitinib) were envisaged for use in therapy of TNBCs because of their excellent performance in other cancer types, such as ovarian and lung cancer (Harbeck and Gluz, 2017). Notably, some clinical trials have investigated the efficacy of regimens using EGFR inhibitors (Costa et al., 2017; Matsuda et al., 2017) and anti-androgen drugs (Denkert et al., 2017).

1.3 Kallikrein-related peptidases

1.3.1 Overview of kallikrein-related peptidases

The term ‘kallikrein’ was first mentioned by Werle et al. (1936) in the 1930s, referring to a kinin-generating substance in the human pancreas. Currently, kallikreins and kallikrein-related peptidases (KLKs) are classified into plasma kallikrein (KLKB1) and the tissue KLK family which encompasses human tissue kallikrein (KLK1) and tissue kallikrein-related peptidases (KLK2–KLK15) displaying 38-79% identical amino acids between each other (Goettig et al., 2010) (**Figure 3**). Only plasma kallikrein (KLKB1) and tissue kallikrein (KLK1) efficiently generate (brady-)kinin cleavage of kininogen, whereas the other members of the tissue KLK family fullfill other functions.

The KLKs are well conserved serine proteases encoded by the largest protease gene cluster of the human genome, located on the long arm of chromosome 19 (19q13.3–19q13.4) (Yousef et al., 2000). The tissue KLKs belong to the serine family S1, which is part of the PA family, displaying chymotrypsin-like or trypsin-like serine protease activity (Yousef et al., 2001). All KLKs are secreted as zymogens, requiring a proteolytic removal of a pro-peptide for activation (Pampalakis et al., 2007). The activation of pro-KLKs forms the basis of a proteolytic network of KLKs interacting with other crucial proteases, e.g. plasmin and matrix metalloprotease (MMP) (Kapadia et al., 2004; Yoon et al., 2013).

For decades, physiological and pathological implications of KLKs have been explored in various tissues and diseases. Indeed, abnormal expression profiles of KLKs have been linked to different tissue-specific disorders including malignancies. In prostate cancer, PSA (KLK3) is used as an essential screening tool and diagnosis biomarker

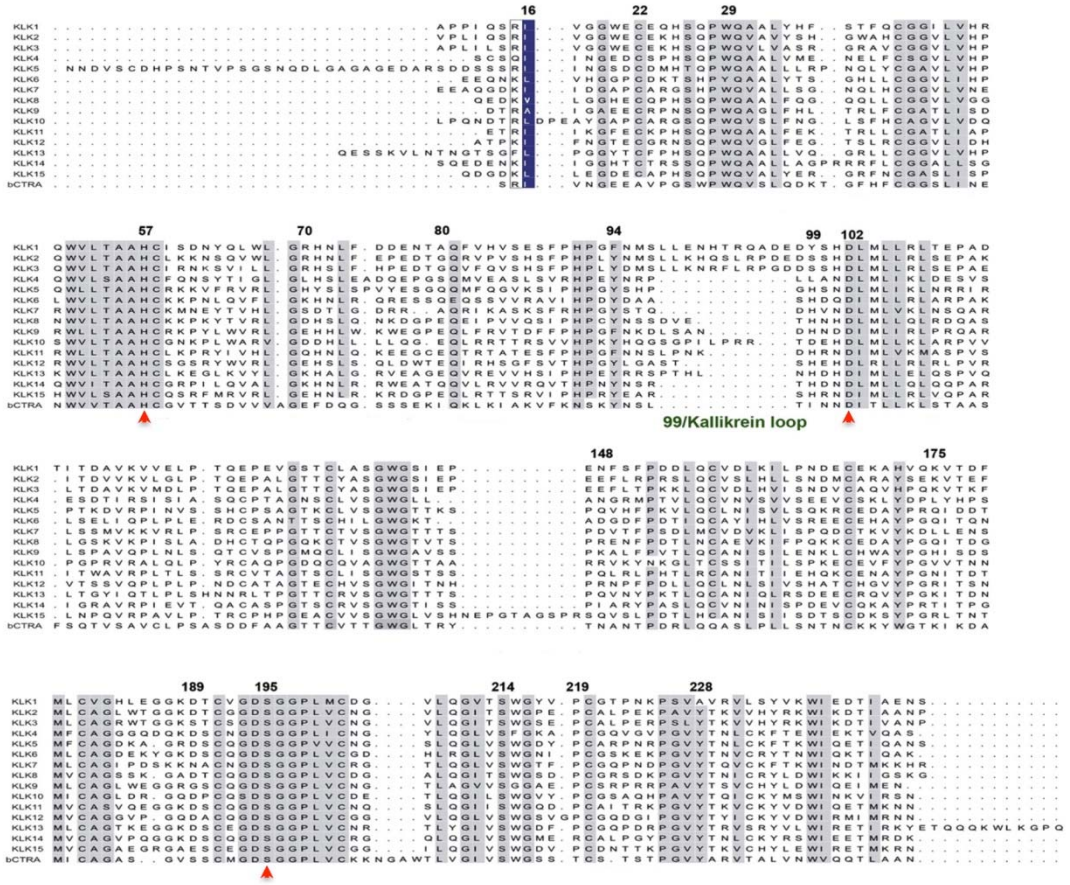

Figure 3. Sequence alignment of tissue kallikrein (KLK1) and the kallikrein-related peptidases (KLK2-15) with bovine chymotrypsin (bCTRA).
The members of the KLK serine protease family share between 38-79% identical amino acids (highly conserved residues are indicated in grey). The family can be subdivided into the so-called classical KLKs (KLK1-3, displaying 61-79% identity with each other) and the so-called new KLKs (KLK4-15 with 38-57% identity), whereby the classical KLKs harbor an extended 99-loop, also called kallikrein loop. The catalytic triad residues (His57, Asp102, and Ser195, according to the bCTRA numbering) are indicated by red arrow heads. The N-terminus of the mature, active enzymes is indicated by the blue box (modified according to Goettig et al., 2010).

based on its elevated expression in prostate tissue. Numerous studies have reported that tumor progression in the prostate is accompanied by an increase in blood levels of PSA (Fleshner et al., 2017; Pinsky et al., 2017). In normal prostate, KLK3 cleaves fibronectin and semenogelin proteins 1 and 2 to accomplish semen liquefaction (Diamandis et al., 1995). Other KLKs, such as KLK2, KLK5, and KLK14, are

postulated to regulate KLK3 activity via their zymogen cascade (Pampalakis et al., 2007). Another case showing disordered expression of KLKs, affects skin epidermis. KLK5 (stratum corneum tryptic enzyme, SCTE), as well as KLK7 (stratum corneum chymotryptic enzyme, SCCE) play an important role in the maintenance of the complete skin barrier (Komatsu et al., 2007a; Komatsu et al., 2007b). Initially, KLK5 in the stratum corneum activates downstream pro-KLK7, as well as pro-KLK8 and pro-KLK14. In turn, stimulated KLK14 triggers proteolytic activation of KLK5, constituting a positive-feedback in the regulation network. Mutations affecting the gene for the serine protease inhibitor Kazal-type 5 (SPINK5) (a main natural inhibitor of KLK5 in the skin) therefore cause an over-stimulated KLK cascade in the skin, which has been identified as the key step of pathogenesis of the severe and lethal Netherton syndrome (NS) (de Veer et al., 2017; Kasparek et al., 2017; Prassas et al., 2015) (**Figure 4**).

1.3.2 KLKs in ovarian cancer

Most members of the KLK family have been reported to be involved in ovarian cancer via modulation of tumor biological processes (Loessner et al., 2018). Furthermore, several KLKs have been demonstrated to function as biological markers of diagnosis and prognosis in ovarian cancer. For example, Ahmed et al. (2016) have assessed mRNA expression levels of KLK6 and KLK8 in tumor tissue of 100 patients afflicted with advanced high-grade serous ovarian cancer. Elevated KLK6 mRNA levels were found to significantly correlate with an approximately two-fold shortened overall survival (OS), independent of other clinical parameters. Although KLK8 mRNA levels were not associated with patient survival, higher KLK6+KLK8 values were significantly linked with worse progression-free survival (PFS). Thus, both KLK6 and, at least in part, KLK8 may be considered as unfavorable prognostic markers and as promising therapeutic targets for ovarian cancer. Moreover, Dettmar et al. (2018) assessed KLK13 and KLK14 mRNA expression levels in tumor tissues of a homogeneous patient cohort afflicted with advanced high-grade serous ovarian cancer.

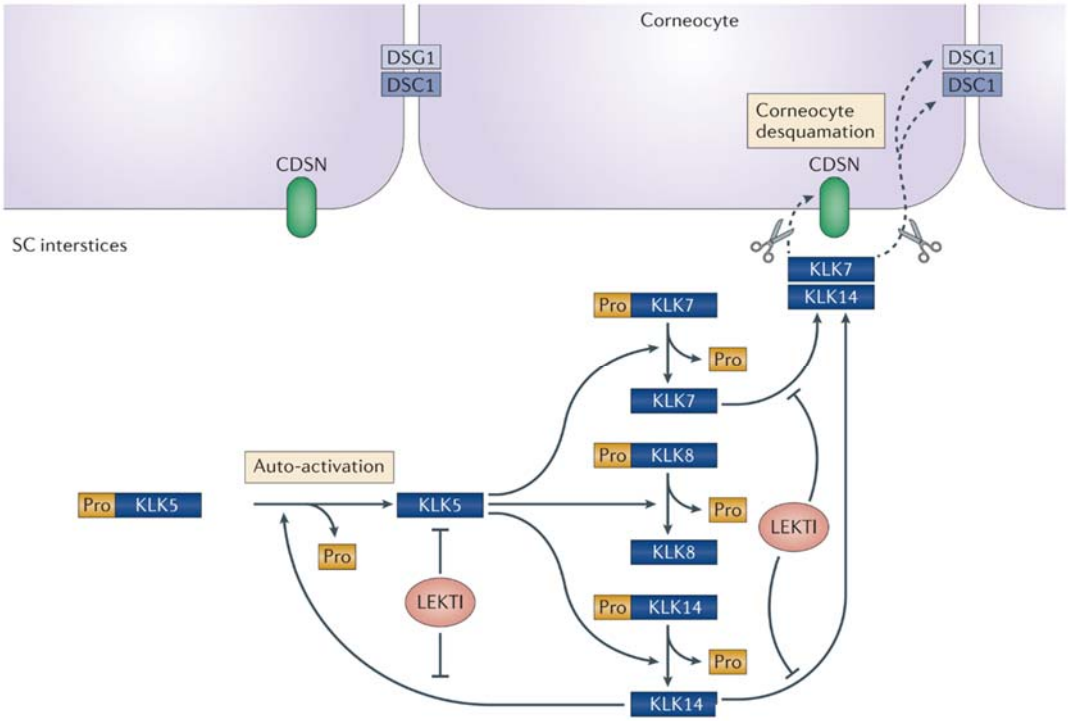

Figure 4. The kallikrein proteolytic cascade in skin epidermis.
Inactive pro-KLK5 is secreted into stratum corneum (SC) interstices to act as the initiator of its auto-activation and then activation of pro-KLK7, pro-KLK8 and pro-KLK14 by removing the pro-peptide (yellow rectangle). In turn, activated KLK14 activates pro-KLK5 through a positive feedback loop. Activated KLK5 and KLK7 cleave corneodesmosomes corneodesmosin (CDSN), desmoglein 1 (DSG1), and desmocollin 1 (DSC1); indicated by the dashed arrows), leading to the shedding of SC corneocyte cells or skin desquamation. The lympho-epithelial Kazal-type-related inhibitor (LEKTI), an epidermal serine-protease inhibitor, inhibits KLK activity in normal and diseased skin. Absence of LEKTI-mediated inhibition of KLK5, KLK7 and KLK14 will over stimulate the cascade which causes Netherton syndrome (NS) (modified according to Prassas et al., 2015).

Elevated KLK13 mRNA levels were reported to significantly correlate with shortened OS and PFS with an approximately two-fold increased risk. Otherwise, higher KLK14 mRNA expression levels were significantly linked to prolonged PFS. The study of Dorn et al. (2016) has assessed KLK5 protein expression levels in tumor tissue microarrays by immunohistochemistry in a cohort of 95 patients suffering from advanced ovarian cancer. Based on a manual semi-quantitative scoring system, elevated KLK5 protein expression levels in stromal cells significantly correlated with prolonged OS and PFS

with a two-fold lower risk for worse outcomes. In another protein study of this group, KLK7 protein expression levels of tumor tissue extracts were assessed by ELISA in a cohort of 98 ovarian cancer patients. In multivariate analyses, patients with elevated KLK7 protein levels showed a significant two-fold lower risk of death (both OS and PFS) compared with those patients having lower KLK7 protein levels (Dorn et al., 2014).

The potential of KLKs as diagnostic biomarkers in ovarian cancer has been explored by numerous studies. A meta-analysis (five studies including 485 ovarian cancer patients, 420 benign ovarian cysts patients and 245 healthy controls) regarding serum protein expression levels of KLK6 reported that a relative high KLK6 expression level was associated with a higher specificity for the diagnosis of ovarian cancer. In line with this finding, high KLK6 levels contributed to an improved diagnosis accuracy of CA125 for the advanced ovarian cancer (Yang et al., 2016). Several other researchers established co-working panels involving KLK6 to improve diagnostic sensitivity and accuracy in ovarian cancer. For example, Leung et al. (2016) suggested a diagnostic panel involving serum protein levels of CA125, KLK6, HE4, and FOLR1, which was based on three individual cohorts encompassing 216 ovarian cancer patients. Overexpression of KLK6 and KLK7 was found in ovarian tumor epithelium rather than in the neighbouring stroma tissues. Moreover, elevated expression levels of both KLKs in serum were linked to specific subtypes of either serous or papillary serous ovarian cancer (Tamir et al., 2014). Dorn and co-workers (2015) proposed a comprehensive score including four KLKs (KLK5, 6, 7 and 13) and other clinical factors (ascites and tumor grades) to identify those ovarian cancer patients who more likely would have a benefit from radical surgery.

1.3.3 KLKs in breast cancer

In breast cancer, expression of several members of KLKs have been shown to be dysregulated as well. In a study encompassing 188 patients afflicted with TNBC, Yang

and co-workers (2017) reported that elevated KLK4 protein expression levels of both tumor cells and stroma cells, detected by immunohistochemistry in primary tumor tissue microarrays, significantly correlated with worse disease-free survival indicating an approximately 2-fold increased relapse risk. Similarly, elevated protein expression levels of KLK5, observed in tumor stromal cells, significantly correlated with distant metastasis and poor clinical outcome in TNBC patients (Yang et al., 2015). Haritos and co-workers (2018) assayed KLK6 mRNA expression levels of tumor specimens in a cohort of 165 breast cancer patients in comparison to 100 adjacent non-cancerous sections. Aberrantly elevated KLK6 mRNA expression levels were suggested to significantly predict a worse disease-free survival of patients (with an approximately 7-fold risk), independent of the routinely used clinical markers (TNM stage, molecular subtype, nodal status, HER2 status, Ki-67 index and age). Moreover, these findings of the differential expression and the prognostic value of KLK6 were validated via *in silico* analyses. Michaelidou and co-workers (2015) assessed KLK8 mRNA expression levels in a group of 150 breast cancer patients in comparison to the KLK8 levels of 100 corresponding normal breast tissue sections. KLK8 mRNA expression was significantly downregulated in cancerous tissues relative to the non-cancerous counterparts. Interestingly, higher KLK8 mRNA expression levels in tumor tissue were significantly associated with an advanced TNM stage (III/IV), a positive nodal status and a shorter disease-free survival (approximately 3-fold risk).

Additionally, KLKs have been involved in multiple levels of breast carcinoma progression. The 36-38bp MSR1 minisatellite element is involved in gene regulation, affecting carcinogenesis of breast cancer. A large number of MSR1 clusters have been found in the KLK gene locus. A MSR1 cluster within the KLK14 locus was identified as the strongest risk factor for so-called non-familiar breast cancer (Rose et al., 2018). In a proteomic analysis of secreted proteins involving 537 patients, serum KLK6 turned out to be one of the top four proteins showing differential expression in over 400 breast carcinoma patients. Elevated serum KLK6 protein levels allowed significant discrimination of invasive breast carcinomas from non-cancerous ones (Mange et al.,

2016). Trastuzumab resistance has emerged as a major issue in treatment practice of breast cancer. In a RNA-Seq analysis in aggressive breast cancer cell lines, KLK10 was identified as a relevant protein which might reverse the trastuzumab resistance of breast carcinoma patients. Therefore, KLK10 could have a potential as a therapeutic target in breast cancer patients resistant to trastuzumab (Wang et al., 2016). In a mass spectrometry study, circulating peptides were explored to identify patients carrying the BRCA1 mutation among breast cancer patients. In the functional peptidases network, the accumulation of protein KNG1K438-R45 significantly discriminated carriers of BRCA1 from those patients that developed breast cancer sporadically. Importantly, serum KLK2 was identified as the key serine protease to cleave and activate KNG1K438-R457 (Fan et al., 2016). Sidiropoulos et al. (2016) reported a KLK6-regulated oncogenic miRNA network which activated oncogenic pathways in breast cancer. Abnormally high expression levels and increased activity of KLK6 were observed in MDA-MB-231 breast cancer cells, which induced alterations of a number of miRNAs (e.g. miR-146a upregulation and/or miR-34a downregulation). Moreover, KLK6 showed significant positive correlations with downstream activation of MAPK and MYC, as well as inhibition of GATA3. Sufficient vitamin D3 uptake is strongly associated with better breast cancer survival. In human breast tumor epithelial cells and clinical samples, a significant KLK6 up-regulation in response to 1 alpha, 25-dihydroxyvitamin D3 (1,25D) treatment was reported among 523 analyzed genes. Moreover, elevated KLK6 levels were associated with prolonged relapse-free survival via changing cellular adhesion, metabolic or tumor suppressor-like pathways (Sheng et al., 2016).

1.3.4 KLK11 and KLK15

KLK11, also termed hippostatin, is highly expressed in normal human tissues including esophagus, skin, salivary gland, and tonsil. In normal ovarian tissue KLK11 showed moderate expression levels of both mRNA and protein, whereas increased expression levels were found in ovarian cancers (Schmitt et al., 2013). In contrast, in breast tissues,

KLK11 showed high expression levels of both mRNA and protein, with no apparent differences compared to breast cancers (Schmitt et al., 2013). Representing a possible tumor-relevant protein, expression of KLK11 has been studied concerning its involvement in tumorigenesis. Jamaspishvili and co-workers (2011) explored the possible association of KLK11 with clinico-pathological parameters of prostate cancer. They reported significantly reduced expression levels of KLK11 in prostate cancer compared to benign prostatic hyperplasia (BPH). Besides, in non-small cell lung cancer (NSCLC), an elevated expression of KLK11 in tumor tissues, as detected by immunohistochemistry, was significantly associated with better overall survival, indicative of KLK11 as a favorable prognostic marker in NSCLC (Unal et al., 2016).

KLK15, also termed prostinogen, is highly expressed in normal human tissues including several endocrine glands (thyroid gland, adrenal gland, and salivary gland), colon, rectum, lung, stomach and testis. As reviewed by Schmitt et al. (2013), KLK15 shows no or rather low expression both concerning mRNA and protein in normal ovarian tissues (Shaw et al., 2007), whereas increased expression levels were found in ovarian cancers. In normal breast tissues, KLK15 mRNA is not detectable, whereas in breast cancer, elevated levels have been found (Schmitt et al., 2013). Moderate KLK15 protein expression has been reported in normal breast tissues, whereas so far no data of breast cancer protein expression have been documented (Schmitt et al., 2013). Because KLK15 is the youngest member of the KLK family, investigation of its role in tumorigenesis is still at its infancy. Nonetheless, a few studies have shown that KLK15 is involved in the progression of malignant diseases. For example, in prostate cancer, KLK15 mRNA expression in 150 tumor specimens was significantly upregulated compared to benign tissue. Elevated levels of KLK15 were statistically associated with advanced stage and with reduced progression-free survival (Mavridis et al., 2013).

2. Objectives

Based on accumulating evidence, the KLK family is suggested to play important roles in tumor-relevant pathological processes. However, the potential of human KLKs to serve as biomarkers for cancer prognosis, still awaits validation studies due to conflicting conclusions. In the present study, we propose that cohorts encompassing different subtypes and stages might contribute - at least in part - to most of the conflicting results. Therefore, we conducted investigations to validate,

1) whether mRNA levels of KLK11 and KLK15 in tumor specimens can predict clinical outcome of advanced high-grade serous ovarian cancer (FIGO III/IV) patients, which is the major subtype (over 70%) of this malignancy;

2) whether KLK11 protein levels in tumor tissue can predict clinical outcome of advanced high-grade serous ovarian cancer (FIGO III/IV) patients;

3) whether an automated digital algorithm can be considered as strategy to assist quantifying protein expression detected by immunohistochemistry;

4) whether KLK11 mRNA levels display an association with clinical outcome of triple-negative breast cancer.

3. Patients, materials and methods

3.1 Patients

Patients with advanced high-grade serous ovarian cancer (FIGO III/IV) and triple-negative breast cancer, treated at the Department of Obstetrics and Gynecology, Klinikum rechts der Isar (Technical University of Munich, Germany) between 1988 and 2014, were enrolled in the present study. The approval of this investigation was accepted by the local Ethics Committee and informed consent in written form was received from every patient. 136 ovarian cancer patients (as cohort 1, **Table 1**), were selected for survival analyses with respect to KLK11 and 15 mRNA expression levels in fresh frozen tumor tissues, whereas 153 patients (as cohort 2, **Table 2**) were included in the study of KLK11 protein expression levels in formalin-fixed, paraffin-embedded tumor tissue. These two cohorts exclusively encompass high-grade serous ovarian cancer (FIGO III/IV) patients with an overlapping number of 54 patients. Concerning TNBC, 108 patients (as cohort 3, **Table 3**) were included in survival analyses regarding KLK11 mRNA expression levels in tumor specimens. Moreover, 60 randomly selected patients afflicted with hormone-receptor positive breast cancers (HPBC) were analyzed for KLK11 mRNA levels for comparison with the triple-negative ones.

3.1.1 High-grade serous ovarian cancer patients (cohort 1)

All ovarian cancer patients initially underwent standard stage-related primary radical debulking surgery, and received adjuvant treatment mainly including platinum-based chemotherapy. None of the patients received any neo-adjuvant therapy prior to primary operation. Clinical parameters documented at the time of surgery included histologic subtype, absence or presence of residual tumor mass after surgery and ascites fluid volume estimated preoperatively by vaginal ultrasound. Five years follow-up times were adapted to assess numbers of events considering relapses and deaths.

In cohort 1, the median patients' age at the time of operation was 64 years (range 33-88 years). 67 patients (49.3%) were optimally debulked with complete removal of all macroscopically visible tumor manifestations. Median follow-up time was 29 months

Table 1. Clinical characteristics of advanced high-grade serous ovarian cancer patients in cohort 1 (n=136)

Clinical parameters	N (%)
Age (years)	
≤ 60	56 (41.2)
> 60	80 (58.8)
FIGO	
III	106 (77.9)
IV	30 (22.1)
Ascitic fluid volume (ml)	
0	34 (25.0)
≤ 500	41 (30.1)
> 500	54 (39.7)
Missing data	7 (5.1)
Residual tumor mass (mm)	
0	67 (49.3)
> 0	67 (49.3)
Missing data	2 (1.5)
Chemotherapy scheme	
Carboplatin + cyclophosphamide (CTX) and/or taxol	80 (58.8)
Carboplatin + taxol + gemcitabine/epirubicin/bevacizumab	28 (20.6)
Only carboplatin	16 (11.8)
Others (no CTX)	5 (3.7)
Missing data	7 (5.1)
Survival time	**Median (range, missing data)**
OS (months)	29 (2-279, 13)
PFS (months)	20 (3-279, 31)

for overall survival (OS, range 2 to 279 months after primary tumor resection) and 20 months for progression-free survival (PFS, range 3 to 279 months). During the follow-up time of 5 years, 74 of 106 (69.8%) patients had relapsed, and 63 of 122 (51.6%) patients had died with available data for PFS and OS.

3.1.2 High-grade serous ovarian cancer patients (cohort 2)

In cohort 2, median patients' age at time of surgery was 65 years (range 33-88 years). 78 patients (51.0%) were optimally debulked with complete removal of all macroscopically visible tumor manifestations. Median time of follow-up was 29 months for overall survival (OS, range 1 to 270 months after primary tumor resection) and 18 months for progression-free survival (PFS, range 4 to 270 months). During the period of five years follow-up, 91 of 126 (72.2%) patients had relapsed, and 68 of 139 (48.9%) patients had died with available data for PFS and OS.

Table 2. Clinical characteristics of advanced high-grade serous ovarian cancer patients in cohort 2 (n=153)

Clinical parameters	N (%)
Age (years)	
≤ 60	55 (35.9)
> 60	98 (64.1)
FIGO	
III	116 (75.8)
IV	36 (23.5)
Missing data	1 (0.7)
Ascitic fluid volume (ml)	
0	37 (24.2)
≤ 500	50 (32.7)
> 500	61 (39.9)
Missing data	5 (3.3)
Residual tumor mass (mm)	
0	78 (51.0)
> 0	71 (46.4)
Missing data	4 (2.6)
Chemotherapy scheme	
Carboplatin + cyclophosphamide and/no taxol	21 (13.7)
Carboplatin/cisplatin + taxol	80 (52.3)
Carboplatin + taxol + gemcitabine/epirubicin/bevacizumab	19 (12.4)
Only carboplatin	12 (7.8)
Others (no CTX)	6 (3.9)
Missing data	15 (9.8)
Survival time	**Median (range, missing data)**
OS (months)	29 (1-270, 14)
PFS (months)	18 (4-270, 37)

3.1.3 Triple-negative breast cancer patients (cohort 3)

In cohort 3 of TNBC, median patients' age at time of surgery was 54 years (range 30-96 years). 61% (66/108) patients were in post-menopausal stage. The major part of cancer concerning histology was invasive ductal type breast cancer (102/108, 94.4%). Distant metastasis existed in cases of 26 patients at the primary diagnosis. Most patients (106/108, 98.1%) initially underwent segment resection or mastectomy surgery. Combined with surgery, patients received adjuvant treatment according to the consensus recommendations at that time. Median time of follow-up was 82.5 months for overall survival (OS, range 4 to 286 months after primary tumor resection) and 77 months for progression-free survival (PFS, range 3 to 269 months). Other clinical and pathological parameters documented at the time of surgery included size of tumor and afflicted nodal status based on TNM staging, respectively. During the follow-up time of 15 years, 32 of 104 (30.8%) patients had relapsed, and 36 of 106 (34.0%) patients had died with available data.

Table 3. Clinical characteristics of triple-negative breast cancer patients in cohort 3 (n=108)

Clinical parameters	N (%)
Age (years)	
≤ 50	46 (42.6)
> 50	62 (57.4)
Menopausal	
Pre-	39 (36.1)
Peri-	3 (2.8)
Post-	66 (61.1)
Histology	
Invasive ductal	102 (94.4)
Invasive tubular/lobar	2 (1.9)
Invasive medullary	2 (1.9)
Others	2 (1.9)
Tumor size	
pT1	32 (29.6)
pT2	61 (56.5)
pT3	6 (5.6)
pT4	9 (8.3)
Nodal status	
pN0	60 (55.6)
pN1	36 (33.3)
pN2	9 (8.3)
pN3	3 (2.8)
Distant metastasis	
No	82 (75.9)
Yes	26 (24.1)

Grading	
G1	1 (0.9)
G2	17 (15.7)
G3	90 (83.3)
Operation type	
Segment resection	70 (64.8)
Mastectomy	36 (33.3)
Others	2 (1.9)
Adjuvant therapies	
Chemotherapy	84 (77.8)
Neo-adjuvant chemotherapy	9 (8.3)
Hormontherapy	17 (15.7)
Radiotherapy	85 (78.7)
Survival time	**Median (range, missing data)**
OS (months)	82.5 (4-286, 2)
PFS (months)	77 (3-269, 3)

3.2 Materials

3.2.1 Reagents and components

Reagents/components	Source	Cat. #
IHC		
Antibody diluent	Zytomed Systems, Berlin, Germany	ZUC025
Citric acid monohydrate	Sigma-Aldrich, St. Louis, USA	C1909
Ethanol	Department of pathology, Technical University of Munich	
Hematoxylin	Dako REAL, Glostrup, Denmark	S2020
Human serum	Department of pathology, Technical University of Munich	
Hydrogen peroxide (30%, H_2O_2)	Roth, Karlsruhe, Germany	9681.4
Isopropanol	Department of pathology, Technical University of Munich	
Pertex	Medite, Burgdorf, Germany	41-4012-00
Sodium chloride (NaCl)	Merck, Darmstadt, Germany	106404
Sodium hydroxide (NaOH)	Roth, Karlsruhe, Germany	T135.1
Trizma base	Sigma-Aldrich, Steinheim, Germany	T1503
Tween-20	Sigma-Aldrich, Munich, Germany	P1379
Xylene	Department of pathology, Technical University of Munich	
qPCR		
KLK11 primers	Metabion, Steinkirchen, Germany	N170314-069
KLK15 primers	Metabion, Steinkirchen, Germany	N160127-020
HPRT primers	Metabion, Steinkirchen, Germany	N170606-154
RLT plus lysis buffer	Qiagen, Oslo, Norway	1053393
TRIzol® LS reagent	Invitrogen, Darmstadt, Germany	10296-010

Acetic acid	Sigma-Aldrich, Munich, Germany	695092
WB		
Rotiphorese® Gel (acrylamide)	Roth, Karlsruhe, Germany	A515
Ammonium persulfate (APS)	Amresco, Solon, USA	C000T82
ECL prime WB detection reagent	Amersham Biosciences, Little Chalfont, UK	RPN2232
PageRuler prestained protein ladder	Thermo Fisher Scientific, Schwerte, Germany	26616
SDS	Carl Roth, Karlsruhe, Germany	0183
Skim milk powder	Sigma-Aldrich, Munich, Germany	70166
TEMED	Omnilab, Munich, Germany	A1148, 0100
Tris hydrochlorid	Roth, Karlsruhe, Germany	9090.3

3.2.2 Kits

Kits	Source	Cat. #
IHC		
Diaminobenzidine (DAB) substrate kit	Zytomed Systems, Berlin, Germany	DAB 5000 plus
ZytoChem plus HPR one-step polymer anti-mouse/rabbit/rat	Zytomed Systems, Berlin, Germany	ZUC053-006/100
PCR		
AllPrep DNA/RNA/miRNA universal kit	Qiagen, Oslo, Norway	80224
Brilliant III ultra-fast qPCR mastermix with low ROX	Agilent Technologies, Böblingen, Germany	600890
Cloned AMV first-strand cDNA synthesis kit	Invitrogen, Darmstadt, Germany	12328040

3.2.3 Consumables

Consumables	Source	Cat. #
IHC		
Microscopical cover slips	R. Langenbrinck, Teningen, Germany	
SuperFrost Plus adhesion microscope slides	Thermo Fisher Scientific, Teningen, Germany	J1800AMNT
PCR		
96-well plate	Agilent, Böblingen, Germany	8010-0534
Collection tube (2 ml)	Qiagen, Oslo, Norway	19201
QIAshredder	Qiagen, Oslo, Norway	79654
Optical cap strip	Agilent, Böblingen, Germany	401425
Presterilized filter tips (1000 µl)	Qiagen, Oslo, Norway	1050173
RNeas-free microfuge tube (2 ml)	Invitrogen, Darmstadt, Germany	AM12425
Safeseal surphob spitzen	Biozym, Hessisch Oldendorf, Germany	VT0210/0220/0260
WB		
PVDF membrane	Carl Roth, Karlsruhe, Germany	T830.1
Glass plates	Biostep, Burkhardtsdorf, Germany	20-30-114

3.2.4 Solutions and buffers

Solutions/buffers		
IHC		
Citrate buffer	H_2O distilled	1 L
	Citric acid monohydrate	2.1 g
	Sodium hydroxide	
	PH	6.0
TBS-T	10×TBS	100 ml
	H_2O distilled	900 ml
	Tween-20	500 µl
Tris-buffered saline (TBS)	Trizma base	60.5 g
	Sodium chloride	90 g
	Distilled H_2O	1 L
	Hydrogen chloride	
	PH	7.6
WB		
Running/electrophoresis buffer	Distilled water to	1 L
	25 mM Tris base	3 g
	10% SDS	10 ml
	1.44% Glycine	14.4 g
Semi-dry buffer	Distilled water	800 ml
	50 mM Tris base	5.82 g
	30 mM Glycine	2.93 g
	0.4% SDS	0.037 g
	Add ethanol to	1 L

3.2.5 Instruments

Instruments	Source
IHC	
Light microscope	Axioskop, Carl Zeiss, Jena, Germany
NanoZoomer digital slide scanner	Hamamatsu Photonics, Hamamatsu, Japan
PH Meter	SCHOTT, Mainz, Germany
Pressure cooker (Ankoch-automatik)	WMF, Munich, Germany
Microm HM355S	Microm GmbH, Walldorf, Germany
PCR	
Centrifuge 5417C	Eppendorf, Hamburg, Germany
Mx3005P qPCR instrument	Agilent Technologies, Böblingen, Germany
NanoDrop 2000/2000c spectrophotometer	Thermo Fisher Scientific, Peqlab, Erlangen, Germany
QIAcube machine	Qiagen, Oslo, Norway
Thermocycler	SensoQuest, Göttingen, Germany
WB	
Molecular imager	Bio-Rad, Munich, Germany
Power pac 300	Bio-Rad, Munich, Germany
Thermomixer 5436	Eppendorf, Hamburg, Germany

3.2.6 Software

Software	Source/websites
IHC	
IHC profiler plugin	Https://sourceforge.net/projects/ihcprofiler
Imagej (Java 1.8.0, 64 bit)	https://imagej.nih.gov/ij
Scanning software NDP 2.0	Hamamatsu Photonics, Hamamatsu, Japan
PCR	
MXPro software 4.10	Agilent, Böblingen, Germany
NanoDrop 2000/2000c software	Thermo Fisher Scientific, Peqlab, Erlangen, Germany

3.3 Methods

3.3.1 RNA extraction

Human ovarian cancer OV-MZ-6 cells which stably over-express either KLK11 or KLK15 (OV-KLK11, OV-KLK15) through stable transfection with pRcRSV-derived expression plasmids encoding the respective pre-pro-proteins (Prezas et al., 2006) were employed as a source of calibrator RNA. Ovarian cancer patients involved in the study were selected from the established Tumor Bank of the Medical Faculty (Technical University of Munich, Germany) based on defined histology and available follow-up information. Deep-frozen tumor tissue samples of enrolled patients, stored in liquid nitrogen, of the tissue storage facility, were picked and sliced into 10 – 20 µg still-frozen tumor material which was immediately dissolved in 600 µl RLT plus lysis buffer containing 1% β-mercaptoethanol. The lysates were directly transferred into a QUIA shredder spin column and placed in a 2 ml collection tube and was thoroughly centrifuged to receive a homogenized flow-through.

Total RNA was isolated from above described lysis solution of cell lines or tumor tissues of ovarian cancer patients. This process was performed by an automated QIAcube sample preparation machine following the manufacturer's instruction of the AllPrep DNA/RNA/miRNA kit. Briefly, first, DNA was purified and eluted with a DNA spin column to obtain flow-through which contained RNA. Then, the RNA solution was supplemented with 150 µl chloroform to purify the solution in case of a high content of fatty tissue in the samples. The purified aqueous phase of RNA solution was separated after thorough vortexing and subsequent centrifugation. In a last step, proteinase K was used to digest left-over protein, DNase I was used for DNA digestion, and ethanol was supplemented to maximize binding of total RNA to the RNA spin column. Afterwards, an optimized RNA clean-up program was performed on the QIAcube machine and RNA was finally eluted in RNase-free water (50 µl). The concentration and quality of isolated RNA were assessed applying the Nano Drop2000c spectrophotometer. The samples with $OD_{260}/OD_{230} > 2$ were selected as qualitied RNA for the experiment. Finally, RNA samples were stored at -80°C until reverse transcription.

3.3.2 Reverse transcription (RT)

RNA reverse transcription was performed using the Invitrogen Cloned AMV first strand synthesis kit. The concentration and quantification of RNA samples were measured by the Nanodrop software. For each sample, input RNA (1000 and 500 ng for cell lines and tumor tissues, respectively) was calculated to mix with hexamer primers as in **Table 4**.

Table 4. RT primer-mix

Component	Each reaction (µl)
Primer (Hexamer)	1
RNA (1000 ng/500 ng)	
DEPC-treated H_2O	Add up to 9
dNTPs	2
Total	12

The established primer mix was denatured at 65°C for 5 min. Preparation of cDNA synthesis buffer was conducted as in **Table 5** and 8 µl of master reaction mix was supplied per reaction system.

Table 5. RT mastermix

Component	Each reaction (µl)
5x cDNA synthesis buffer	4
0.1 MDTT	1
DEPC-treated H_2O	1.1
RNase OUT (40 U/µl)	1
Cloned AMV RT (15 units/µl)	0.9
Total	8

The reverse transcription program was run in thermal cycler with definite temperatures and times in **Table 6**. Finally, cDNA samples were diluted (end-volume: 100 µl) with RNase free water.

Table 6. Reverse transcription reaction

Step	Temperature (°C)	Time (min)
1	25	10
2	50	50
Termination	85	5
Preservation	4	Unlimited

3.3.3 Quantitative real-time polymerase chain reaction (qPCR)

Specific primers were designed with the Universal Probe Library (UPL) assay (https://lifescience.roche.com/products/universal-probelibrary-system-assay). Details of used primers and hydrolysis probes from UPL are shown in **Table 7**.

Table 7. qPCR primers (5'-3')

Gene	Forward	Reverse	UPL probe
KLK11	GCTTGCTCT	AGTGAGGCTT	54
	GGCAACAGG	GCACTCGAAC	GAGACCAG
KLK15	TCCCTCATC	GTGGTCCGTA	14
	TCCCCACACT	GTTGCTCTGG	CTTCCTGC
HPRT1	TGACCTTGATTT	CGAGCAAGAC	73
	ATTTTGCATACC	GTTCAGTCCT	GCTGAGGA

The assay detects mRNA transcript variants 1 and 2 of KLK11, variants 2, 3 and 4 of KLK15, which all encode the full length protein of the respective gene. The Taqman-based technology (FAM-labelled UPL Taqman probes) with brilliant III qPCR master mix with low ROX was selected. A 20 µl reaction system containing 15 ng of patients' cDNA sample (30 ng cDNA for calibrators) was established with components shown in **Table 8**. To figure out false-positive results, a no-template sample (RNA-free water) and a no-RT sample (patient sample treated with RT process without Cloned AMV RT) were used as negative controls. The results representing different mRNA expression levels were normalized based on the hypoxanthine-guanine phosphoribosyltransferase

(HPRT) expression level of each sample and calibrator (mRNA of OV-KLK11 and OV-KLK15 for KLK11, KLK15, respectively) expression level in each run.

Table 8. qPCR mastermix (20 µl system)

Component	Concentration (µM)	Each reaction (µl)	Final conc. (nM)
RNAase free H_2O		5.8	
Brilliant III		10	
Primer forward	20	0.4	400
Primer reverse	20	0.4	400
UPL probe	10	0.4	200
cDNA sample		3	
Total		20	

The assay of each sample was performed in 96-well plates in triplicates on the Mx3005P qPCR machine using the MXPro software 4.10 (standard settings). The cycling program was performed following **Table 9**. The cycle threshold (Ct) values were automatically determined by reading fluorescent signals during amplification cycles, accompanied by adaptive correction of baseline and threshold value.

Table 9. qPCR cycles

Segment	Cycle	Temperature (°C)	Duration
Denaturation	1	95	3 min
Annealing	40	95	15 s
Elongation		60	1 min

Detector: Taq; Reference dye: ROX

In a pretest, standard dilution series were conducted to compare the amplification efficiency of KLK11 and KLK15 with that of the control housekeeping gene HPRT (Bustin and Nolan, 2013). Establishment of standard dilution curves for KLK11, KLK15, and HPRT was performed using cDNA samples of both cell lines (OV-KLK11 and OV-KLK15) diluted into 5 concentration levels based on a 2-fold dilution gradient

(DNA0-DNA4; range 30-1.875 ng). The dilution curves were depicted using each dilution concentration (x-variable) against the threshold cycle value (y-variable) via linear regression analysis. The efficiency (E) was calculated by following formula:

$$E = 10\exp(-1/\text{Slope})$$

exp: exponential function

An E value of 2 corresponds to 100% efficiency. A R^2 coefficient was analyzed to represent the quality of the regression curves. Three repeated dilution tests validated the stable amplification efficiency of KLK11/KLK15 which corresponded to that of control HPRT, thereby the delta E between target KLK11/KLK15 gene and HPRT was calculated showing acceptable efficiency related error margins. One run of dilution series curves for KLK11 and KLK15 respectively are shown in **Appendix Figure 15** to display details.

Due to the ideal approximation of KLK11/HPRT and KLK15/HPRT amplification efficiency, the relative target gene expression was estimated by directly calculating 2ΔΔCt (Pfaffl, 2012), as in this formula:

$$\Delta\Delta Ct = \Delta Ct_{sample} - \Delta Ct_{calibrator}$$

$$\Delta Ct = Ct_{target} - Ct_{HPRT}$$

Where, relative error propagation (EP) was calculated as in formula:

$$EP(\Delta Ct) = \sqrt{(STDEV_{marker}{}^2 + STDEV_{HPRT}{}^2)/2}$$

$$EP(\Delta\Delta Ct) = \sqrt{(STDEV_{\Delta Ct\ (sample)}{}^2 + STDEV_{\Delta Ct\ (calibrator)}{}^2)/2}$$

$$Absolute\ error = \ln 2 \times EP(\Delta\Delta Ct) \times 2 - \Delta\Delta Ct_{sample}$$

STDEV: standard deviation; ln: natural logarithm

Due to limitations and variables of the detection system, quality criteria were applied. Uncertain results were excluded if one of the following conditions existed: Ct (HPRT) > 35; error progression % of 2exp (-ΔΔCt) > 30% even after repetition; and % STDEV of 2exp-(ΔΔCt) > 47.1% in two separate valid runs.

3.3.4 Western blotting (WB)

The specificity of the antibody used in immunohistochemistry was tested via Western blotting. In brief, full length proteins of KLK11-15, made in-house, were used to test the antibody specificity. PageRuler prestained protein ladder was applied as size standard. Polyacrylamide (PAA) gels were prepared as in **Table 10**.

Table 10. Components of acrylamide gels

Separating gel (12%)		**Stacking gel (5%)**	
Component	**Volume**	**Component**	**Volume**
Distilled water	6.6 ml	Distilled water	17.2 ml
1.5M Tris-Cl (pH 8.8)	3.75 ml	0.5M Tris-Cl (pH 6.8)	7.2 ml
10% SDS	0.15 ml	10% SDS	0.28 ml
40% Acrylamide	4.5 ml	40% Acrylamide	3.6 ml
10% APS	80 µl	10% APS	50 µl
TEMED	8 µl	TEMED	10 µl

After separation by electrophoresis, target proteins were transferred to polyvinylidene difluoride (PVDF) membrane via semi-dry blotting method. The primary antibody specifically targeting KLK11 protein (**Table 11**) was supplied in blocking buffer to incubate PVDF membrane overnight.

Table 11. Primary antibody detected KLK11

Target gene	Description	Source	Cat. #	Dilution
KLK11	Polyclonal rabbit IgG (0.5 mg/ml)	Abcam	ab131038	1:1000 (WB) 1:500 (IHC)

Afterwards, the membrane was incubated with horseradish peroxidase (HRP)-coupled secondary antibody (1:5000). Potential protein bands were visualized using enhanced chemilumescent (ECL) substrates detection reagents and exposure to X-ray films. The detailed process protocol of Western blotting is given in **Table 12**.

Table 12. Western blotting protocol

- Preparation of protein samples (40 µg protein + 10 µl loading buffer)
- Denaturation of samples at 95°C for 5 min, afterwards kept on ice
- Preparation for stacking and separating polyacrylamide gels as in **Table 10**
- Addition of the loading solution of each sample to the gel, and the PageRuler prestained protein ladder as the control marker
- SDS polyacrylamide gel electrophoresis (SDS-PAGE) in running buffer to achieve concentration (90 V, about 30 min) and separation (120 V, about 1 h) of the proteins
- Transfer of the proteins to a PVDF membrane via semi-dry blotting in glycine buffer (75 mA, about 2 h)
- Washing the PVDF membrane in 15 ml TBST with gentle shaking (3x5 min)
- Blocking unspecific antibody via incubation in 5% skim milk blocking buffer (RT, 1 h)
- Incubation with the primary antibody detected to KLK11, diluted in 10 ml blocking buffer (4°C, overnight, with gentle agitation)
- Washing membranes in 15 ml TBST with soft shaking (3x10 min)
- Incubation with HRP-coupled secondary antibody (1:5000) in 1% milk TBST (RT, 1 h)
- Washing membrane in 15 ml TBST with soft shaking (3x10 min)
- Incubation with the mixture of ECL detection reagents (1:1) for 1 min
- Visualization by exposure as X-ray films on imager machine with optimized time

3.3.5 Construction of tissue microarray

Tissue specimens of ovarian cancer patients were collected from the archives of the Pathology Institute (Technical University of Munich, Germany). Tumor tissue microarrays (TMA) were constructed by members of the Clinical Research Unit of the Women's Hospital and the Institute of Pathology, following previously established and practiced guidelines by Wan and coworkers (Wan et al., 1987; Skacel et al., 2002). Briefly, first of all, tumor biopsies of ovarian cancer patients were resected in surgery with careful inspection from a trained pathologist, then immediately fixed in neutral formalin buffer before embedded in paraffin. Afterward, HE stained slides were routinely prepared for each individual patient's sample. Upon analyzing these sections, areas representing typical tumor morphology were marked by the pathologist. By orientation of HE staining results, three cylindrical core biopsies in 1 mm diameter were picked out and carefully removed from each paraffin-embedded donor block. On a manual tissue microarray device, tumor cores were precisely positioned into empty holes of a paraffin recipient block prepared in advance according to predefined templates. Additionally, various tissues from healthy adult donors of the archives were used as controls. To set up TMA slides for specific staining detection, 2 μm-thick layers of the recipient block were sliced by a standard routine microtome and displayed on an electrostatically charged glass slide. A total of 13 TMAs were assembled with 153 patients' samples were constructed and chosen as database for the assay of KLK11 protein expression levels in ovarian tumor tissues.

3.3.6 Immunohistochemistry (IHC)

An assay protocol for staining was optimized and, finally, a polymer one-step-based system for KLK11 protein detection in ovarian cancer tissues was used. Details of the protocol are shown in **Table 13** including major steps: antigen retrieval via pressure cooking in citrate buffer (pH 6.0, 4 min), quenching endogenous peroxidase activity with 3% hydrogen peroxide (room temperature, 20 min), reaction of polyclonal rabbit antibodies directed to KLK11 (Abcam ab131038, 1:500, 4°C, overnight), and visualization using the polymer secondary antibody based on a horseradish peroxidase-

linked reporter assay.

Table 13. Polymer one-step system protocol

- Deparaffination and rehydration:
3 x 10 min xylol, 2 x isopropanol, 1 x 96% alcohol, 1 x 70% alcohol, each 5 min
- Washing in TBST buffer, with intervening buffer changes, 5 min
- Blocking in 3% hydrogen peroxide (30%, 45 ml distilled water + 5 ml H_20_2) (RT, 20 min)
- Washing in normal tap water, 2 min
- Washing in TBST buffer, with intervening buffer changes, 5 min
- Pressure cooking in citrate buffer, pH 6.0, 4 min
- Washing in normal tap water, 5 min
- Washing in TBST buffer, with intervening buffer changes, 5 min
- Primary antibody incubation using a polyclonal anti-rabbit antibody detecting KLK11
(abcam ab131038, 1:500, 4 °C, overnight)
- Washing in TBST buffer, with intervening buffer changes, 5 min
- Polymer complex incubation (Zytomed, RT, 30 min)
- Washing in TBST buffer, with intervening buffer changes, 5 min
- Visualization with DAB substrate (1000 µl buffer + 50µl substrate, per 8 slides, RT, 8 min)
- Washing in TBST buffer, with intervening buffer changes, 5 min
- Counter-staining with haematoxylin, 60 s
- Washing under flowing normal tap water, 10 min
- Transfer into distilled water, 1 min
- Dehydration
70% alc, 96% alc, 2 x isopropanol, 2 x xylol, each 3 min
- Cover-glass with pertex

RT: room temperature; alc: alcohol (etoh)

3.3.7 Quantification of immunostaining

In the present study, a semi-quantitative automated method was used applying the publicly available free software *ImageJ* (Java 1.8.0, 64 bit, downloaded from *https://imagej.nih.gov/ij*) combined with a so-called *IHC Profiler* plugin (downloaded from *https://sourceforge.net/projects/ihcprofiler/*). Scanned RGB (red, green, blue) digital images of whole stained sections were documented employing the NDP 2.0 software. Selected images of each tumor tissue core were uploaded to the *ImageJ* analysis platform with 5× amplification. The color deconvolution to separate the DAB staining signal from the rest of the images was performed by incorporation of the plugin *IHC Profiler*. The principle and procedure of utilizing the plugin for IHC analysis were explained by researchers before (Varghese et al., 2014). The default setting threshold was used when analyzing DAB signals and the cytoplasmic protein pattern was selected. Typical areas of tumor cells picked for quantification analysis were chosen by observation of two individual researchers. An immunoreactive score (IRS) as continuous variable for statistical analysis was calculated by following formula:

$$Score = 255 - \sum_{i=1}^{n} InD_i \Big/ \sum_{i=1}^{n} A_i$$

InD: integrated gray density

A: area (unit, pixel)

The semi-quantified system follows the Lambert-Beer law (Commoner and Lipkin, 1949), in which the optical density (OD) is proportional to the concentration of a light-absorbing substance, in this case the color. When the integrated optical density is averaged over the whole area, the mean staining intensity is obtained, reflecting the staining intensity of the target KLK11 protein. This score ranges from 0 to 255 where 0 represents the darkest staining shade and 255 represents the lightest. Therefore, a subtraction was performed which assists the IRS to be positively associated with the protein expression levels. For each patient, three individual tissue cores were examined to get the average IRS.

To validate this digital algorithm, a previously established manual quantitative score was applied to quantify the immunostaining intensity of KLK11 in tumor cells as well (Dorn et al., 2016). This score was based on the observation of pathologist for staining intensity and percentage of positive cells. KLK11 staining intensity was evaluated on a scale of 0 to 3 (0: no staining; 1: weak staining; 2: moderate staining; 3: strong staining). The percentage of positive cells was counted on a scale of 0 to 4 (0: 0%; 1: 1-10%; 2: 11-50%; 3: 51-80%; 4: > 80%) (Biesterfeld et al., 1996). This manual immunoreactivity score was finally calculated by multiplying the intensity values with the positive cell values for tumor cells.

3.3.8 Statistical analyses

Standard dilution series curves were depicted by linear regression analysis for calculating the efficiency (E) values. The association of KLK mRNA/protein expression levels with respective to clinical factors of ovarian/breast cancer was estimated by the Chi-square test. The prognostic values of KLK markers and pathological factors in prediction of patients' clinical outcomes were analyzed by univariate/multivariate Cox regression models using hazard ratio (HR) combined with a 95% confidence interval (95% CI). Survival curves were depicted by Kaplan-Meier analysis, applying the log-rank test for statistical difference. In survival analyses, overall survival (OS) and progression-free survival (PFS) were restricted to respective time periods as end-up events. In multivariate Cox regression analyses, base models were established by clinical parameters of ovarian cancer (age, residual tumor size, and pre-operative ascites fluid volume) and breast cancer (age, menopausal status, tumor size, and nodal status), respectively. The association of the KLK11 digital immunoreactivity score and the pathologist's immunoreactivity score was examined by Spearman analysis. The difference of KLK11 mRNA levels between TNBC and HPBC patients was evaluated by independent samples t test. All statistical analyses were performed with the software SPSS 20.0. P-values ≤ 0.05 were considered as being statistical significant.

4. Results

4.1 Clinical relevance of KLK11 and KLK15 mRNA expression levels in advanced high-grade serous ovarian cancer patients

4.1.1 KLK11 and KLK15 mRNA expression and their relation to patients' tumor characteristics

For analysis of KLK11 and KLK15 mRNA expression, patient cohort 1 (n = 136; for details see **Table 1**) was used. This cohort exclusively encompasses patients afflicted with advanced high-grade serous ovarian cancer. The mRNA expression levels in primary tumor tissues were determined by the newly established qPCR systems (for details see **Materials and Methods**). Most samples showed robust KLK11 mRNA expression (range 0 to 78.34, median 6.97), while generally low KLK15 mRNA expression levels were observed (range 0 to 25.35, median 0.074, **Figure 5**).

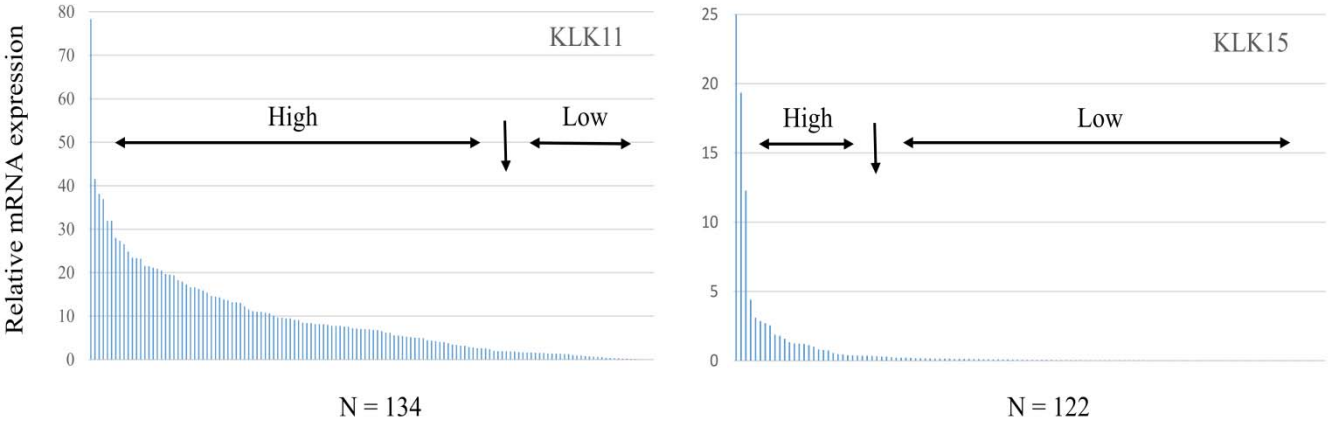

Figure 5. Robust KLK11 mRNA expression and generally low KLK15 mRNA expression levels are detected in tumor tissues of advanced high-grade serous ovarian cancer patients.
The histograms display relative mRNA expression profiles of KLK11 and KLK15 normalized to HPRT by qPCR. For further analyses, the levels were dichotomized into low- and high-expression groups by the following cut-offs: KLK11 = 25th percentile, KLK15 = 75th percentile.

For survival analyses, cut-offs were defined to dichotomize low- and high-expression groups, in case of KLK11 by the 25th percentile (quartile (Q) 1 *vs.* Q2+3+4), and for

KLK15 by the 75th percentile (Q1+2+3 *vs.* Q4), respectively. Based on this categorization, the association between KLK mRNA expression levels and the established clinical parameters (age ≤ 60 *vs.* > 60 years, pre-operative ascites fluid volume ≤ 500 *vs.* > 500 ml, and post-operative residual tumor mass 0 *vs.* > 0 mm) was analyzed. Both KLK11 and KLK15 mRNA expression levels showed no significant association with any of these clinical parameters (**Table 14**).

Table 14. Association between clinical characteristics of advanced ovarian cancer patients (FIGO III/IV) and KLK11/15 mRNA expression

Clinical parameters	KLK11 Low/high	KLK15 Low/high
Age (years)	p = n.s.	p = n.s.
≤ 60	11/45	36/15
> 60	22/56	53/18
Residual tumor mass (mm)	p = n.s.	p = n.s.
0	17/48	45/17
> 0	16/51	43/15
Ascitic fluid volume (ml)	p = n.s.	p = n.s.
≤ 500	21/52	51/18
> 500	11/43	33/14

Cohort number = 136;
Cut-off: KLK11 = 25th percentile, KLK15 = 75th percentile;
Chi-square test, $p < 0.05$ is considered as statistically significant.

4.1.2 Association of KLK11 and KLK15 mRNA expression with overall (OS) and progression-free (PFS) survival in univariate analysis

The prognostic values of KLK11 and KLK15 mRNA expression levels and clinical parameters indicating patients outcome, overall and progression-free survival within a 5-years observed time, were analyzed by univariate Cox regression analysis. Concerning the clinical parameters, residual tumor mass (post debulking surgery) as well as a high volume of pre-operative ascites fluid were significantly associated with both shorter OS and PFS. Notably, increased KLK11 mRNA levels were found to significantly correlate with both longer OS (HR = 0.53, 95% CI = 0.31 - 0.91, $p = 0.021$) and PFS (HR = 0.49, 95% CI = 0.29 – 0.83, $p = 0.008$), representing an about two-fold decreased probability of death/relapse risk in patients with high KLK11 expression. Moreover, increased KLK15 mRNA values showed a trend towards significance, indicating longer OS (HR = 0.55, 95% CI = 0.30 – 1.03, $p = 0.060$) (**Table 15**).

Table 15. Univariate Cox regression analysis of clinical outcome in advanced ovarian cancer patients (FIGO III/IV) with respect to clinical parameters and KLK11/15 mRNA expression

Clinical parameters	OS			PFS		
	No[a]	HR (95% CI)[b]	*p*	No[a]	HR (95% CI)[b]	*p*
Age (years)			n.s.			n.s.
≤ 60	48	1		41	1	
> 60	74	1.32 (0.79-2.21)		64	1.22 (0.76-1.97)	
Residual tumor mass (mm)			**< 0.001**			**< 0.001**
0	61	1		56	1	
> 0	59	3.86 (2.19-6.81)		49	2.55 (1.59-4.08)	
Ascitic fluid volume (ml)			**0.014**			**0.021**
≤ 500	69	1		60	1	
> 500	46	1.92 (1.14-3.21)		39	1.77 (1.09-2.87)	
KLK11 mRNA			**0.021**			**0.008**
low	30	1		23	1	
high	90	0.53 (0.31-0.91)		80	0.49 (0.29-0.83)	
KLK15 mRNA			*0.060*			n.s.
low	78	1		70	1	
high	30	0.55 (0.30-1.03)		26	0.67 (0.39-1.15)	

Available data for prognosis: OS = 122, PFS = 105;
[a] No: number of patients;
[b] HR: hazard ratio, CI: confidence interval;
Cut-off: KLK11 = 25th percentile, KLK15 = 75th percentile;
Significant values ($p < 0.05$) are indicated in bold, trends towards significance are indicated in italics.

Kaplan-Meier survival analysis, representing another univariate assay, was performed to validate and visualize these findings via depicting respective survival curves. Similar to the Cox regression analysis, increased KLK11 mRNA levels were found to be significantly associated with both longer OS ($p = 0.018$) and PFS ($p = 0.006$), whereas KLK15 mRNA levels retained a trend towards significance in OS analysis ($p = 0.055$) (**Figure 6**).

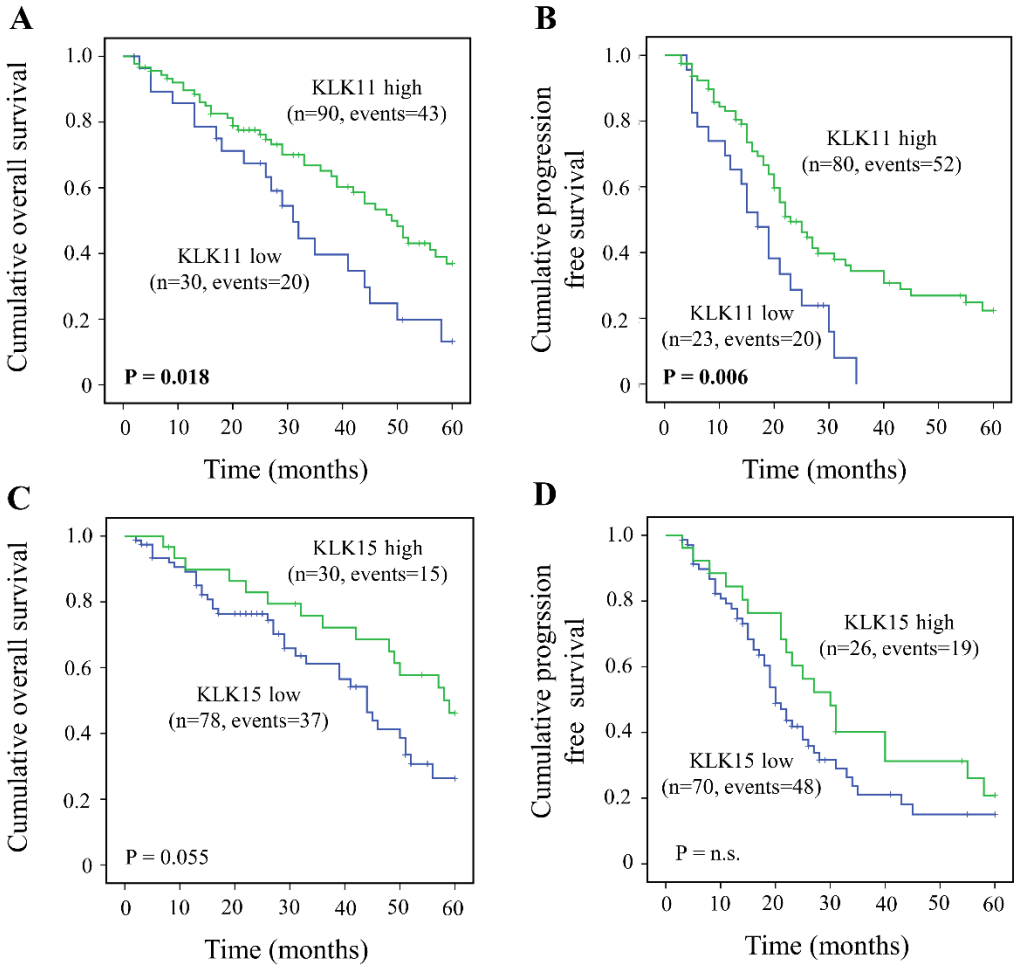

Figure 6. Higher KLK11 mRNA expression levels indicate significantly better clinical outcomes of advanced high-grade serous ovarian cancer patients.
Kaplan-Meier survival curves show probability of 5-years overall survival and progression-free survival of patients with respect to KLK11 and KLK15 mRNA expression levels in primary tumor tissues, respectively. Elevated KLK11 mRNA expression levels significantly correlate with longer OS (A, $p = 0.018$) and PFS (B, $p = 0.006$). KLK15 mRNA levels show a trend towards significance in case of OS (C, $p = 0.055$), but not PFS (D).

Subsequently, a publicly available Affymetrix database of ovarian cancer patients was used to validate the findings concerning KLK11 and KLK15 mRNA expression levels and prognosis (Gyorffy et al., 2012). The microarray-assessed gene expression data and patients follow-up information originate from The Cancer Genome Atlas (TCGA) and the Genomic Spatial Event (GSE). Analogously to our patient cohort, only patients with an advanced stage (FIGO III/IV), high-grade (grade 3), serous subtype, and platinum-based chemotherapy were selected for 5-years survival analyses. A total of 705 patients for OS and 681 patients for PFS assessment were identified. The Kaplan-Meier plotter was conducted as assessment tool to analyze for survival differences. The cut-off was set at the 25th percentile (Q1 *vs.* Q2+3+4) to dichotomize low- *versus* high-expression groups, which matches the cut-off used in our study. In fact, the favorable prognostic value of higher KLK11 mRNA levels was confirmed for both OS (logrank $p = 0.014$) and PFS (logrank $p = 0.015$) (**Figure 7**). However, KLK15 mRNA expression was not associated with both OS and PFS (data not shown).

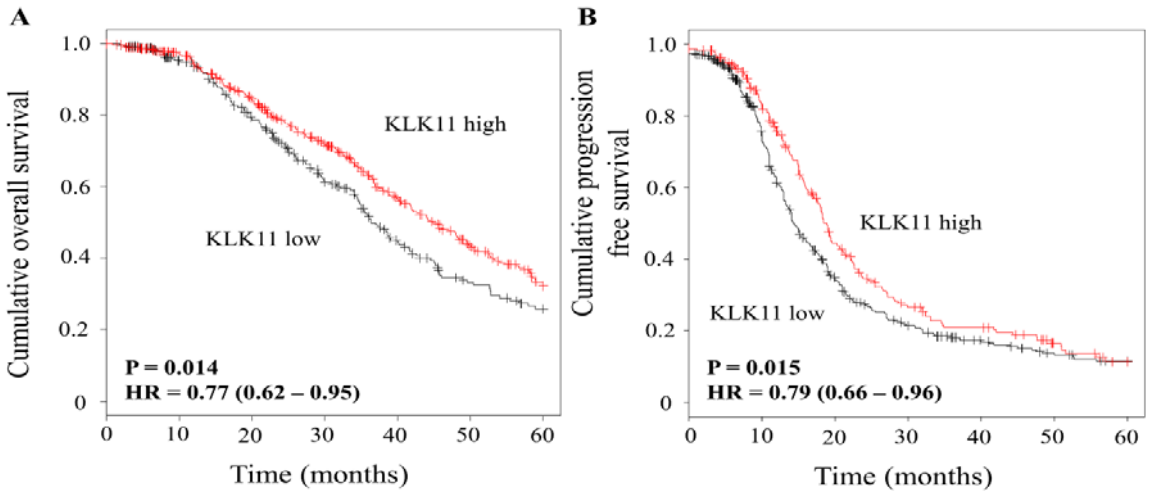

Figure 7. The significant prognostic value of KLK11 mRNA expression levels in advanced high-grade serous ovarian cancer patients is confirmed in a publicly available microarray dataset.
Kaplan-Meier survival curves show the probability of 5-years overall survival and progression-free survival of patients with respect to KLK11 mRNA expression levels (Affymetrix probe set ID 205470_s_at). Elevated KLK11 mRNA expression levels significantly correlate with longer OS (A, $p = 0.014$, HR = 0.77) and PFS (B, $p = 0.015$, HR = 0.79).

4.1.3 Association of KLK11 and KLK15 mRNA expression with overall (OS) and progression-free (PFS) survival in multivariable analysis

To study the independence of the prognostic value of KLK11/15 mRNA expression, a multivariable Cox hazard regression analysis was performed for OS and PFS estimation (5-years observed time). A base model was established including the clinical parameters age, ascites fluid volume, and residual tumor mass. When adjusted to the multivariable model, residual tumor mass remained as the only clinical factor which significantly predicted a shorter OS (HR = 3.72, 95% CI = 1.84 – 7.50, $p < 0.001$) and PFS (HR = 2.14, 95% CI = 1.24 – 3.69, $p = 0.006$), whereas ascites fluid volume turned out to lose its significance in predicting OS and PFS. When included in the base model, KLK11 mRNA expression levels maintained significance correlating with both better OS (HR = 0.40, 95% CI = 0.20 – 0.78, $p = 0.007$) and PFS (HR = 0.47, 95% CI = 0.26 – 0.86, $p = 0.015$). When the biological factor KLK15 mRNA expression was separately added to the base model, it turned out to be independently associated with longer OS (HR = 0.46, 95% CI = 0.23 – 0.91, $p = 0.025$) (**Table 16**). Similarly, when both KLK11 and KLK15 were simultaneously added to the base model, KLK11 remained a significant marker for better OS and PFS, and KLK15 for OS (data not shown).

Table 16. Multivariable Cox regression analysis of clinical outcome in advanced ovarian cancer patients (FIGO III/IV) with respect to clinical parameters and KLK11/15 mRNA expression

Clinical parameters	OS			PFS		
	No[a]	HR (95% CI)[b]	*p*	No[a]	HR (95% CI)[b]	*p*
Age (years)			n.s.			n.s.
≤ 60	40	1		36	1	
> 60	58	1.46 (0.79-2.71)		52	1.07 (0.63-1.83)	
Residual tumor mass (mm)			**< 0.001**			**0.006**
0	53	1		49	1	
> 0	45	3.72 (1.84-7.50)		39	2.14 (1.24-3.69)	
Ascitic fluid volume (ml)			n.s.			n.s.
≤ 500	60	1		54	1	
> 500	38	1.09 (0.55-2.18)		34	1.26 (0.71-2.25)	
KLK11 mRNA			**0.007**			**0.015**
low	25	1		19	1	
high	73	0.40 (0.20-0.78)		69	0.47 (0.26-0.86)	
KLK15 mRNA			**0.025**			n.s.
low	70	1		63	1	
high	28	0.46 (0.23-0.91)		25	0.70 (0.40-1.24)	

KLK11/15 mRNA were separately added to the base model (age, residual tumor mass, and ascitic fluid volume);

[a] No: number of patients;

[b] HR: hazard ratio, CI: confidence interval;

Cut-off: KLK11 = 25th percentile, KLK15 = 75th percentile;

Significant values ($p < 0.05$) are indicated in bold.

4.2 Clinical relevance of KLK11 protein expression levels in advanced high-grade serous ovarian cancer patients

4.2.1 KLK11 protein expression and its relation to patients' tumor characteristics

For analysis of KLK11 protein expression, patient cohort 2 (n = 153; for details see **Table 2**) was used encompassing exclusively patients afflicted with advanced high-grade serous ovarian cancer. KLK11 protein expression levels in tumor specimens were assessed by immunohistochemistry. The specificity of the primary antibody detecting KLK11 protein was validated showing no cross-reaction to the other KLKs (**Figure 8**).

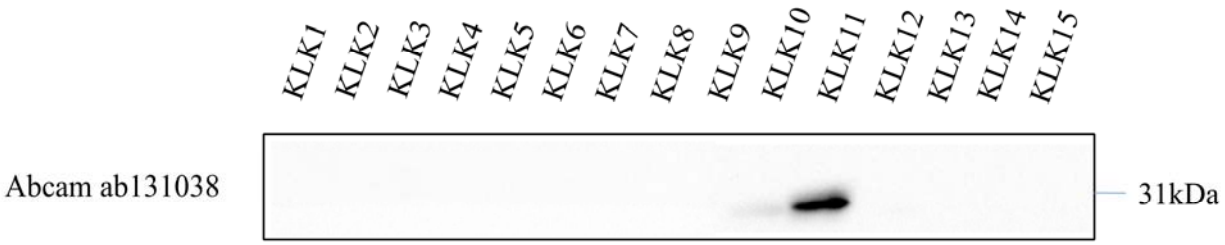

Figure 8. Specificity of the primary antibody directed to KLK11 is confirmed by Western blot analysis.
Recombinantly expressed KLK1-15 proteins were applied as samples. The polyclonal rabbit antibody directed to KLK11 (Abcam ab131038) was used. A specific signal is exclusively visualized in the position of KLK11 protein with no cross-reaction to the other KLKs (The faint signal visible in the KLK10 lane is very likely due to a slight contamination doing application of these samples onto the SDS-gel).

A relative quantitative immunoreactive score (IRS) was determined for each of the samples based on an automated digital algorithm (for details see **Materials and Methods**). Most samples displayed robust cytoplasmic KLK11 protein expression (**Figure 9**) in tumor cells (IRS values ranging from 40.96 to 159.92, median 96.29) (**Figure 10**). Stromal cell-associated KLK11 staining was also detected in endothelial and highly inflammatory stroma cells, e.g. fibroblasts and immune cells.

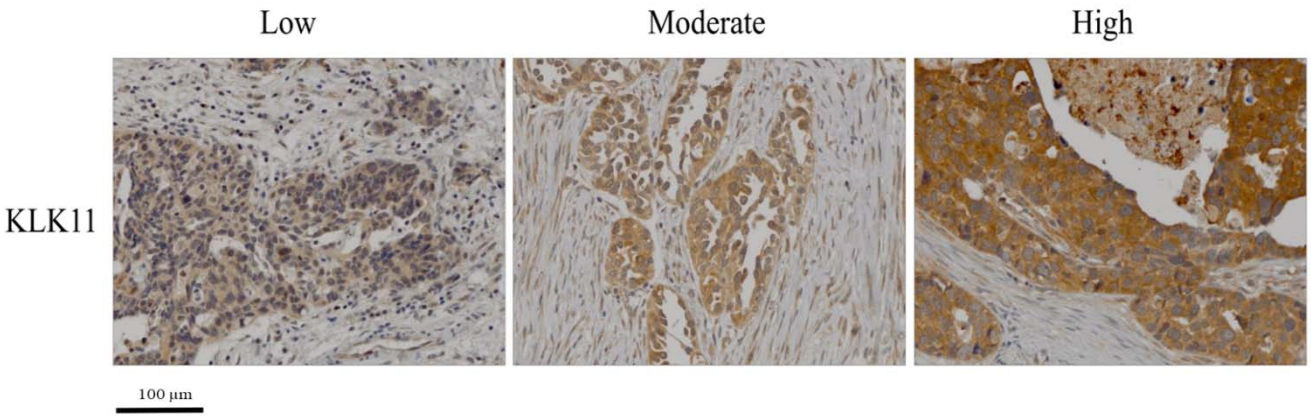

Figure 9. KLK11 protein expression in tumor cells of advanced high-grade serous ovarian cancer patients' specimens.

Tumor tissue microarrays were stained with a specific primary antibody directed to KLK11 (polyclonal rabbit, Abcam ab131038). The polymer one step system based on a horseradish peroxidase-linked reporter assay was applied. Based on the automated relative immunoreactive score, micrographs showing representative core punches are displayed corresponding to low, moderate, and high KLK11 staining intensity levels in tumor cells, respectively. Scale bar: 100 µm.

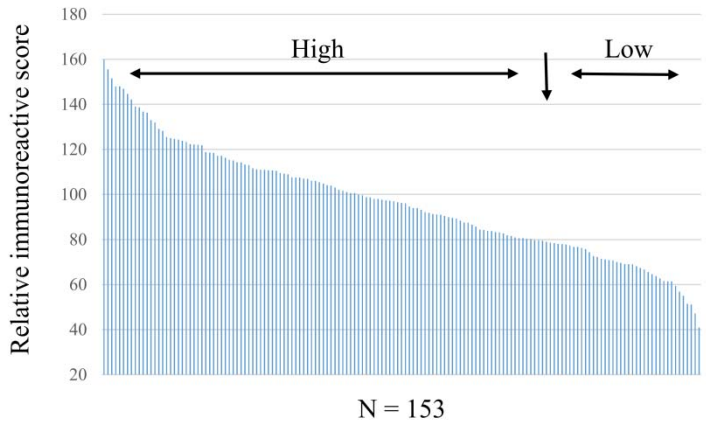

Figure 10. Robust protein expression levels of KLK11 are observed in tumor cells of advanced high-grade serous ovarian cancer patients.

The histogram displays the relative protein expression profile of KLK11 based on specific immunohistochemical staining and digital scoring. For further analyses, the levels were dichotomized into low- and high-expression groups by the cut-off at the 25th percentile.

Moreover, this digital algorithm was validated by our previously established scoring system performed by pathologists (for details see **Materials and Methods**). In the overlapping patients (n = 151), using the manual scoring values, low (0 ≤ IRS < 7), moderate (7 ≤ IRS < 10) and high (10 ≤ IRS ≤ 12) expression levels of KLK11 were observed in 13.9% (21/151), 53.0% (80/151), and 33.1% (50/151) of the cases, respectively. The manual scores significantly correlated with the digital scores (Spearman, R = 0.594, $p < 0.001$, **Figure 11**).

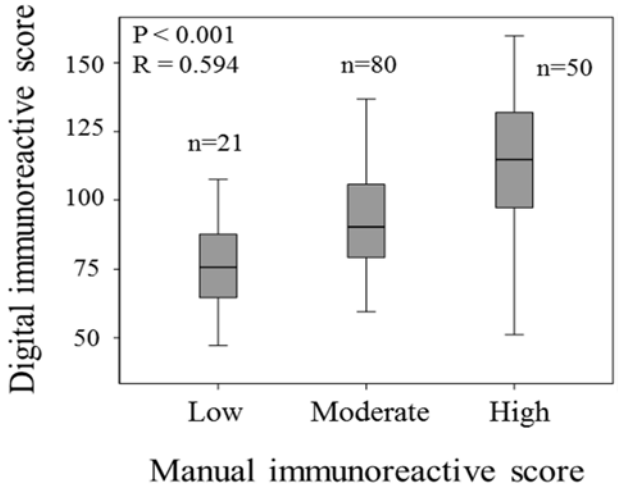

Figure 11. Correlation of two immunoreactive scores for evaluating KLK11 protein expression in tumor tissues.
The digital scores are significantly associated with the manual score. A digital algorithm applying the software *Imagej* (range 0-255), as well as a manual scoring method performed by pathologists (range 0-12) were used (for details see **Materials and Methods**). The manual immunoreactive scores were divided into low (0 ≤ IRS < 7, n = 21), moderate (7 ≤ IRS < 10, n = 80) and high (10 ≤ IRS ≤ 12, n = 50) expression groups for analyzing their association with the digital immunoreactive score (Spearman, R = 0.594, $p < 0.001$).

For survival analyses, a cut-off at the 25th percentile (Q1 *vs.* Q2+3+4) was defined to dichotomize a low- *versus* high-expression group which matches the cut-off for KLK11 mRNA expression used in cohort 1 (**Figure 10**). No associations between KLK11 protein expression levels and established clinical parameters were found (**Table 17**).

Table 17. Association between clinical characteristics of advanced ovarian cancer patients (FIGO III/IV) and KLK11 protein expression

Clinical parameters	KLK11 Low/high
Age (years)	*p* = n.s.
≤ 60	12/43
> 60	26/72
Residual tumor mass (mm)	*p* = n.s.
0	19/59
> 0	18/53
Ascitic fluid volume (ml)	*p* = n.s.
≤ 500	22/65
> 500	16/45

Cohort number = 153;
Cut-off: KLK11 = 25th percentile;
Chi-square test, $p < 0.05$ is considered as statistically significant.

4.2.2 Association of KLK11 protein expression with overall survival (OS) in univariate analysis

Similarly to the mRNA study, the prognostic value of KLK11 protein expression levels as well as of clinical parameters as indicators for patients' clinical outcomes (5-years OS and PFS) was analyzed by univariate Cox regression analysis. Residual tumor mass after surgery and a high volume of pre-operative ascites fluid, respectively, were significant unfavorable markers for both OS and PFS. Consistent with the findings concerning mRNA, increased KLK11 protein expression levels were significantly associated with longer OS (HR = 0.56, 95% CI = 0.34 – 0.93, $p = 0.025$), representing

an about two-fold decreased probability of death risk in 5 years for the patients showing higher KLK11 protein expression (**Table 18**).

Table 18. Univariate Cox regression analysis of clinical outcome in advanced ovarian cancer patients (FIGO III/IV) with respect to clinical parameters and KLK11 protein expression

Clinical parameters	OS		
	No[a]	HR (95% CI)[b]	*p*
Age (years)			n.s.
≤ 60	50	1	
> 60	89	1.29 (0.78-2.13)	
Residual tumor mass (mm)			**< 0.001**
0	69	1	
> 0	66	3.99 (2.31-6.89)	
Ascitic fluid volume (ml)			**0.026**
≤ 500	80	1	
> 500	54	1.74 (1.07-2.82)	
KLK11 IRS			**0.025**
low	36	1	
high	103	0.56 (0.34-0.93)	

Available data for prognosis: n = 139;
[a] No: number of patients;
[b] HR: hazard ratio, CI: confidence interval;
Cut-off: KLK11 = 25th percentile;
Significant values ($p < 0.05$) are indicated in bold.

No significant association was observed between KLK11 protein levels and PFS. The Kaplan-Meier analysis (OS; $p = 0.022$) is depicted in **Figure 12**.

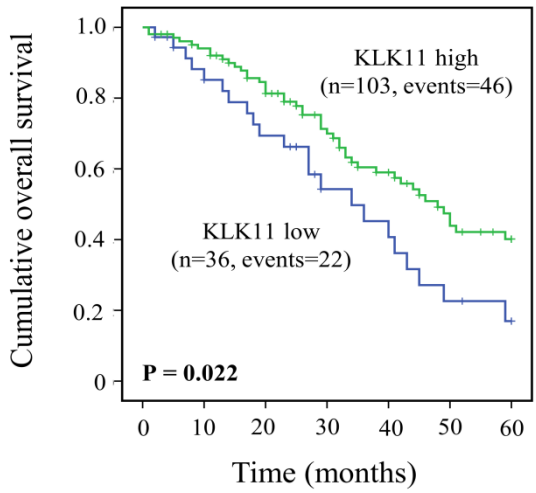

Figure 12. Higher KLK11 protein expression levels indicate significantly better clinical overall survival in advanced high-grade serous ovarian cancer patients. Kaplan-Meier survival curves show the probability of 5-years overall survival of patients with respect to KLK11 relative protein expression levels in primary tumor tissue specimens. Elevated KLK11 protein expression levels significantly correlate with longer OS ($p = 0.022$). $p < 0.05$ indicates significance in bold.

4.2.3 Association of KLK11 protein expression with overall survival (OS) in multivariable analysis

To study the independence of the prognostic value of KLK11 protein expression, a multivariable Cox hazard regression analysis was performed. Analogously to the analysis of mRNA expression, first, a base model was established. Here, the parameter "residual tumor mass" performed as the only significant predictor for shorter OS (HR = 3.61, 95% CI = 2.01 – 6.48, $p < 0.001$), whereas the parameter "ascites fluid volume" lost its significance. Importantly, KLK11 protein expression levels remained as an independent prognostic marker, displaying a significant association of elevated KLK11 levels with better OS (HR = 0.55, 95% CI = 0.32 – 0.95, $p = 0.031$) (**Table 19**).

Table 19. Multivariable Cox regression analysis of clinical outcome in advanced ovarian cancer patients (FIGO III/IV) with respect to clinical parameters and KLK11 protein expression

Clinical parameters	OS		
	No[a]	HR (95% CI)[b]	*p*
Age (years)			n.s.
≤ 60	48	1	
> 60	83	0.89 (0.52-1.54)	
Residual tumor mass (mm)			**< 0.001**
0	67	1	
> 0	64	3.61 (2.01-6.48)	
Ascitic fluid volume (ml)			n.s.
≤ 500	78	1	
> 500	53	1.19 (0.70-2.01)	
KLK11 IRS			**0.031**
low	35	1	
high	96	0.55 (0.32-0.95)	

KLK11 IRS was added to the base model (age, residual tumor mass, and ascitic fluid volume);
[a] No: number of patients;
[b] HR: hazard ratio, CI: confidence interval;
Cut-off: KLK11 = 25th percentile;
Significant values ($p < 0.05$) are indicated in bold.

4.3 Clinical relevance of KLK11 mRNA expression levels in triple-negative breast cancer patients

4.3.1 KLK11 mRNA expression and its relation to patients' tumor characteristics

For analysis of KLK11 mRNA expression in TNBC, patient cohort 3 (n = 108; for details see **Table 3**) which exclusively encompasses patients afflicted with triple-negative breast cancer was used. The mRNA expression levels in primary tumor tissues were determined by the qPCR system established for analysis of KLK11 mRNA in HGSOC (for details see **Materials and Methods**). Most samples show low KLK11 mRNA expression levels (ranging from 0.00 to 2.70, median 0.01) (**Figure 13**).

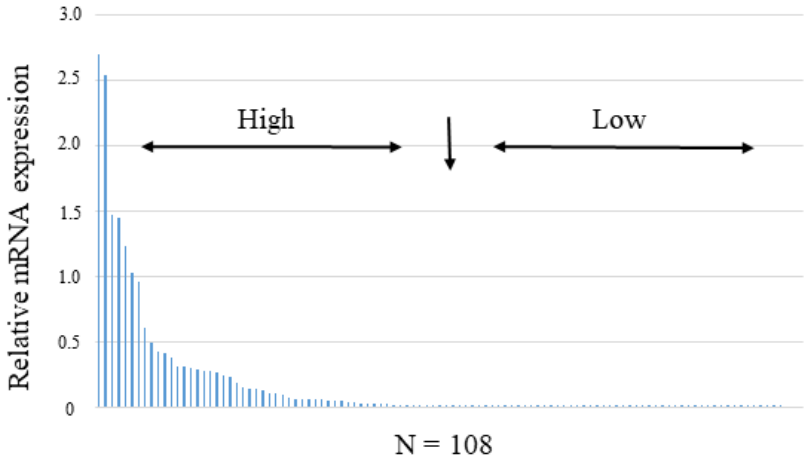

Figure 13. Relative low mRNA expression levels of KLK11 are observed in tumor tissues of triple-negative breast cancer patients.
The cumulative histogram displays the relative mRNA expression profile of KLK11 normalized to HPRT determined by qPCR. For further analyses, the levels were dichotomized into low- and high-expression groups by the median.

In addition, 60 stochastically selected tumor samples of hormone receptor-positive breast cancers were also analyzed for KLK11 mRNA expression levels to compare the KLK11 expression pattern with that in TNBC. Most samples showed low expression of KLK11 mRNA (ranging from 0.00 to 2.31, median 0.004) as well. KLK11 mRNA expression of these hormone-receptor positive breast cancer patients was not significantly different from those of TNBC (**Appendix Figure 16**).

For survival analyses, the cut-off was defined by the median (Q1+2 *vs.* Q3+4) to dichotomize low- and high-expression groups. Based on this categorization, the associations between KLK11 mRNA expression levels and the established clinical parameters (age ≤ 50 *vs.* > 50 years, pre- and peri-menopausal status *vs.* post-menopausal status, tumor size pT1 *vs.* pT2+pT3+pT4, nodal status pN0 *vs.* pN1+pN2+pN3, and nuclear grade G1+G2 *vs.* G3) were analyzed. No significant correlation was found between KLK11 mRNA expression levels with any of these clinical parameters (**Table 20**).

4.3.2 Association of KLK11 mRNA expression with overall survival (OS) in univariate analysis

The clinical relevance of KLK11 mRNA expression levels and clinical parameters concerning OS (15-years observation time) was analyzed by univariate Cox regression analysis. Age over 50 years and post-menopausal status significantly correlated with worse overall survival, indicating about 3-fold elevated risk of death in both cases. Concerning KLK11, increased mRNA expression levels showed a trend towards significance correlating with shorter OS (HR = 1.95, 95% CI = 1.00 – 3.82, $p = 0.052$), representing an about two-fold increased probability of death risk in the patients possessing higher KLK11 mRNA expression levels (**Table 21**). However, when the prognostic value for OS was examined by Kaplan-Meier survival analysis, a significant result ($p = 0.047$) was obtained. When the observed time was not restricted to 15 years, KLK11 mRNA expression was associated with OS as well ($p = 0.031$) (**Figure 14**).

Table 20. Association between clinical characteristics of triple-negative breast cancer patients and KLK11 mRNA expression

Clinical parameters	KLK11 Low/high	*p*
Age (years)		n.s.
≤ 50	21/25	
> 50	33/29	
Menopausal status		n.s.
Pre/peri	20/22	
Post	34/32	
Tumor size		n.s.
pT1	14/18	
pT2+pT3+pT4	40/36	
Nodal status		n.s.
pN0	32/28	
pN1+pN2+pN3	22/26	
Nuclear grade		n.s.
G1+G2	7/11	
G3	47/43	

Cohort number = 108;
Cut off: KLK11 = median;
Chi-square test, $p < 0.05$ is considered as statistically significant.

Table 21. Univariate Cox regression analysis of clinical outcome in triple-negative breast cancer patients with respect to clinical parameters and KLK11 mRNA expression

Clinical parameters	OS180		
	No[a]	HR (95% CI)[b]	*p*
Age (years)			**0.005**
≤ 50	44	1	
> 50	62	3.24 (1.42-7.41)	
Menopausal status			**0.010**
Pre/peri	40	1	
Post	66	3.18 (1.32-7.65)	
Tumor size			n.s.
pT1	32	1	
pT2+pT3+pT4	74	1.43 (0.65-3.14)	
Nodal status			n.s.
pN0	58	1	
pN1+pN2+pN3	48	1.67 (0.86-3.23)	
Nuclear grade			n.s.
G1+G2	18	1	
G3	88	0.99 (0.41-2.37)	
KLK11 mRNA			*0.052*
low	52	1	
high	54	1.95 (1.00-3.82)	

Available data for prognosis: n = 106; [a] No: number of patients; [b] HR: hazard ratio, CI: confidence interval; Cut-off: KLK11 = median; Significant values ($p < 0.05$) are indicated in bold, trends towards significance are indicated in italics.

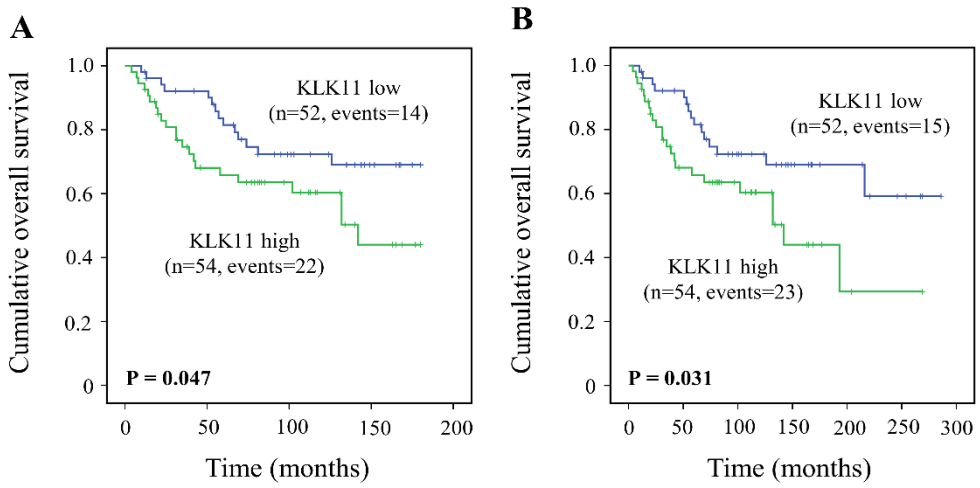

Figure 14. Higher KLK11 mRNA expression levels indicate significantly worse clinical overall survival in triple-negative breast cancer patients.
Kaplan-Meier survival curves show probability of 15-years and all time overall survival in patients with respect to KLK11 mRNA expression levels in primary tumor tissues. Elevated KLK11 mRNA expression levels significantly correlate with unfavorable OS (A, observation time: 15 years, $p = 0.047$; B, maximum observation time, $p = 0.031$). $p < 0.05$ indicates significance in bold.

4.3.3 Association of KLK11 mRNA expression with overall survival (OS) in multivariable analysis

To study the independence of the prognostic value of KLK11 mRNA expression, multivariable Cox hazard regression analysis was performed. A multivariable base model was established including the clinical factors age, menopausal status, tumor size, and nodal status. In this model, only age displayed a trend towards significance as a predictor for shorter OS (HR = 2.70, 95% CI = 0.88 – 8.31, $p = 0.084$), whereas menopausal status lost its prognostic value. Notably, upon addition to the base model, elevated KLK11 mRNA levels turned out to be significantly associated with shorter OS (HR = 2.02, 95% CI = 1.02 – 3.99, $p = 0.044$) (**Table 22**).

Table 22. Multivariable Cox regression analysis of clinical outcome in triple-negative breast cancer patients with respect to clinical parameters and KLK11 mRNA expression

Clinical parameters	OS180		
	No[a]	HR (95% CI)[b]	*p*
Age (years)			*0.084*
≤ 50	44	1	
> 50	62	2.70 (0.88-8.31)	
Menopausal status			n.s.
Pre/peri	40	1	
Post	66	1.36 (0.41-4.52)	
Tumor size			n.s.
pT1	32	1	
pT2+pT3+pT4	74	1.39 (0.63-3.09)	
Nodal status			n.s.
pN0	58	1	
pN1+pN2+pN3	48	1.44 (0.73-2.81)	
KLK11 mRNA			**0.044**
low	52	1	
high	54	2.02 (1.02-3.99)	

KLK11 mRNA was added to the base model (age, menopausal status, tumor size, and nodal status);
[a] No: number of patients;
[b] HR: hazard ratio, CI: confidence interval;
Cut-off: KLK11 = median;
Significant values ($p < 0.05$) are indicated in bold, trends towards significance are indicated in italics.

5. Discussion

In the present study, we assessed the prognostic potential of two tumor-relevant KLKs, KLK11 and KLK15, in two different malignant diseases. First, the tumor tissue-associated mRNA expression levels of KLK11 and KLK15 were examined in a homogeneous patient cohort afflicted with advanced high-grade serous ovarian cancer (FIGO III/IV). Second, the protein expression levels of KLK11 were investigated in tumor specimens from a collection of tissue microarrays, using a homogeneous patient cohort afflicted with advanced high-grade serous ovarian cancer (FIGO stage III/IV). Third, the mRNA levels of KLK11 were quantified in tumor tissue of a homogeneous patient cohort suffering from triple-negative breast cancer (TNBC). In all cases, the clinical relevance of KLK11 and/or KLK15 expression for the different patients' cohorts was estimated by survival analyses, respectively.

Previous studies have demonstrated increased mRNA levels of KLK11 in ovarian cancer tissue compared to normal tissue (Borgoño et al., 2003; Schmitt et al., 2013). In normal ovary, KLK11 mRNA expression levels are low (Loessner et al., 2018). Yousef and co-workers (2003) have analyzed gene expression patterns of 15 KLKs applying the Cancer Genome Anatomy databases and revealed an upregulation of KLK11 in both cancerous ovarian tissues and cell lines. Moreover, elevated serum levels of KLK11 were proposed to allow the distinction between ovarian cancer patients and healthy controls (McIntosh et al., 2007). In the present study, we detected both robust mRNA and protein expression levels of KK11 in tumor tissue of patients afflicted with advanced ovarian cancer (for details see **Figure 5** and **Figure 10**), indicating a possible relationship between KLK11 expression and the progression of ovarian carcinomas.

Concerning KLK15, upregulation of mRNA levels in ovarian tumor tissue has been observed previously (Loessner et al., 2018; Schmitt et al., 2013). Already in 2003, in a study analyzing 168 patients afflicted with epithelial ovarian cancer, significantly higher expression levels of KLK15 mRNA were found in cancerous tissues compared

to benign tissues (Yousef et al., 2003). In the study presented here, we found a rather low expression pattern of KLK15 mRNA in about 75% patients of the advanced high-grade serous ovarian cancer (for details see **Figure 5**). It is of note, however, that normal ovary has no expression of KLK15 mRNA at all (Loessner et al., 2018).

In a study analyzing 20 human cancer cell lines (Sano et al., 2007), two estrogen receptor positive (ER+) breast cancer cell lines (MCF-7 and T47D) showed the highest KLK11 levels. However, KLK11 was not expressed in the two estrogen-independent breast cancer cell lines (MDA-MB231 and MDA-MB468). Similarly, Paliouras et al. (2008) found an upregulation of KLK11 following androgen stimulation in the human breast cancer cell line T47D. Both studies showed an elevated KLK11 expression in human breast cancer cells upon hormone stimulation. In line with these observations, in our study, relatively low expression levels of KLK11 mRNA were detected in TNBC tissue specimens (for details see **Figure 13**). However, no significant differential KLK11 expression was observed in TNBC specimens compared to the tumor tissues of hormone-receptor positive (ER+ and/or PR+, 60 cases) breast cancer patients (for details see **Appendix Figure 16**).

However, as discussed above, it is well established that the expression of KLKs is regulated by steroid hormones (Borgoño et al., 2004; Sano et al., 2007). Shaw and Diamandis (2008) have analyzed the impact of steroid hormones on KLK expression in 32 cancer cell lines. In their study, KLK11 was upregulated by several steroid hormones, e.g. estrogen, dexamethasone, androgen and/or progestin in breast cancer cell lines. KLK15 expression levels were increased by estrogen in prostate cancer cells. Additionally, co-regulation of KLKs including KLK11, appeared to be induced by steroid hormones. For instance, KLK6, 10 and 11 were co-upregulated by dexamethasone in MCF-7 cells, and KLK6, 11 and 14 were all upregulated by estradiol in BT-474 cells (Clarkson et al., 2006). Therefore, it is reasonable to speculate that hormone-related mechanisms are, at least in part, involved in the KLKs' regulation cascade of KLK11/15 in ovarian and/or breast cancer. To validate the expression level

of KLK11 in breast cancer and its relation to its regulation by steroid hormones, further studies analyzing larger clinical cohorts and detailed analysis of the role of hormones in gene regulation are required.

In the present study, we observed that higher KLK11 mRNA levels in tumor tissue were significantly associated with both longer overall survival (OS) and progression free survival (PFS) of patients with advanced high-grade serous ovarian cancer (for details see **Figure 6** and **Table 15, 16**). Moreover, this prognostic value of KLK11 mRNA was independent of established clinical parameters of ovarian cancer (for details see **Table 14**). We validated these findings with an online microarray dataset which is publicly available (for details see **Figure 7**). Furthermore, higher KLK11 protein level significantly performed as a favorable marker for OS in another patient group afflicted with high-grade serous ovarian cancer (for details see **Figure 12** and **Table 18, 19**). The favorable value of elevated KLK11 expression in high-grade serous ovarian cancer (FIGO III/IV) both on the mRNA and protein levels, as detected in the present study, is consistent with findings of previous studies. Diamandis et al. (2004) reported that women with elevated KLK11 protein expression in ovarian tumor extracts showed a significantly prolonged OS and PFS. Similarly, Borgoño et al. (2003) reported that elevated KLK11 protein levels in ovarian tumor cytosolic extracts correlated more frequently with a less aggressive subtype and therefore significantly with favorable OS and PFS. However, also some controversial reports have been published over the past years with regard to the prognostic value of KLK11. For example, Shigemasa et al. (2004) have demonstrated that increased KLK11 mRNA levels were associated with poor prognosis of patients suffering from epithelial ovarian cancer. The varying results of these studies can probably be explained by the fact that quite heterogeneous cohorts were used in all of these studies. In the study of Shigemasa et al. (2004), mRNA analysis was conducted in a small, heterogeneous cohort (n = 64). Only 26 patients were of the serous subtype and about half of the samples were categorized as early stage ovarian cancer (FIGO I/II). In the study of Borgoño et al. (2003) encompassing 104 ovarian cancer patients, only approximately 50% of the patients were of the serous subtype (n

= 53) and a more aggressive stage (n = 69, FIGO III/IV). In the study by Diamandis et al. (2004), 102 of the analyzed 134 ovarian cancer patients were at an advanced stage and 95 patients belonged to the serous subtype.

Concerning KLK15, the present study showed that elevated KLK15 mRNA levels displayed a trend towards an association with longer OS of high grade serous ovarian cancer patients (for details see **Figure 6** and **Table 15)**, and this impact turned out to be significant and independent in multivariable analysis (for details see **Table 16**). However, Yousef et al. (2003) have reported that increased expression of KLK15 is associated with reduced OS and PFS in ovarian cancer patients. Again, a rather inhomogeneous cohort was analyzed consisting of 45% (76/168) patients diagnosed with a serous subtype and of about 30% cases categorized as tumor grade 1/2. Thus, if the KLK15 mRNA expression differs between ovarian cancer subtypes and/or low *versus* high grade tumors, inconsistent results may be obtained, depending on the composition of the cohort. Therefore, for verification of the clinical relevance of KLK11 and 15 expression levels in ovarian cancer, additional studies focusing on a specific carcinoma subtype are needed.

The clinical relevance of KLK11 and KLK15 has been explored for various other cancer types. Wen and co-workers (2011) determined KLK11 mRNA and protein levels in 400 gastric cancer patients, and found that elevated KLK11 expression was significantly associated with well-differentiated tumor cells and lower distant-metastasis risk after primary gastrectomy. In contrast, Kolin and co-workers (2016) assessed KLK11 protein levels of 113 gastric cancer specimens by immunohistochemistry and reported that higher KLK11 protein levels were significantly associated with shorter overall survival. In another study, Xu and colleagues (2014) examined serum KLK11 protein values of 138 non-small cell lung cancer patients and revealed a significant relationship of elevated KLK11 levels with both longer OS and PFS. Aside from survival outcome, KLK11 was proposed as a useful biomarker concerning assessment of other clinical parameters in cancer. For example, in colorectal cancer, for patients with synchronous

liver metastasis, Lu and co-workers (2013) established a predictive model which incorporated KLK11 for evaluation of response sensitivity to FOLFOX4 chemotherapy. In gastric cancer patients, positive KLK11 protein expression significantly indicated a more sensitive response to chemoradiotherapy, contributing to a favorable prognosis (Unal et al., 2013). Furthermore, in laryngeal cancer, upregulation of KLK11 mRNA expression was associated not only with inhibition of tumor growth but also with repressed angiogenesis (Patsis et al., 2012). Taken together, KLK11 has been proven as a promising cancer biomarker and the present study found the convincing potential of KLK11 as a favorable prognosis marker for advanced serous ovarian cancer patients.

Regarding KLK15, the clinical relevance has not been sufficiently explored compared to KLK11. Previous studies pointed to a possible correlation of KLK15 expression with progression of some hormone-related carcinomas. For example, Yousef et al. (2001) reported that the steroid hormone-induced upregulation of KLK15 mRNA was associated with a more aggressive phenotype in LNCaP prostate cancer cells. In prostate tumor tissue samples of 90 patients, Stephan et al. (2003) found significantly higher KLK15 mRNA expression levels in advanced prostate cancerous tissues (pT3/4) compared to the less aggressive ones (pT2). In breast cancer, Yousef et al. (2002) analyzed KLK15 mRNA levels in 202 breast carcinoma tissues. Here, higher KLK15 levels independently predicted prolonged OS and PFS in patients afflicted with lower grade, oestrogen-receptor negative, and progesterone-receptor negative tumors. These studies support the clinical potential of KLK15, since it performed as a prognostic biomarker in advanced ovarian cancer. Again, it is important to analyze a larger homogeneous patient cohort to validate these results.

The possible regulatory mechanism of KLK11 and 15 in ovarian cancer is yet not as clear as for KLK11 in breast cancer. The classical proteolytic network of KLKs may be involved in the progression regulation of KLK11/15 in ovarian and/or breast cancer. The KLK family encompasses the largest continuous cluster of proteases in the human genome (Pavlopoulou et al., 2010). Due to the chromosomal co-localization, KLKs are

often coordinately expressed in various diseases (Sotiropoulou et al., 2009). The cross-activating cascade of KLK pro-forms is stimulated by mature KLKs (Goettig et al., 2010). Activities of KLKs can be induced and enhanced by autolytic, reciprocal, cross-activated, and reverse-activated proteolysis (Cassim et al., 2002; Brattsand et al., 2005), as well as by other endopeptidases. For example, pro-KLK11 is efficiently activated by KLK4 and 5 (Beaufort et al., 2010). Yoon et al. (2007) reported that mature KLK11 represents a broad activator for other KLKs. The authors analyzed hydrolysis of pro-KLK1–15 fusion proteins by mature KLK11 via mass spectrometry. They showed that pro-KLK1, 3–6, 9, and 11–15 fusion proteins were significantly hydrolyzed by mature KLK11. In addition, KLK15 exhibited significant activation of proteases pro-KLK8 and 14 (Yoon et al., 2009). The so-called thrombostasis axis was found to be associated with KLKs cascades as well, again using the fusion-protein system of KLK pro-peptides for analysis. Pro-KLK11 was reported to be activated by several members of this axis, e.g. plasmin, thrombin, and uPA (Luo et al., 2006; Yoon et al., 2008). Yoon et al. (2008) further demonstrated that MMP-8, as well as MMP-2, acted specifically as activator of pro-KLK15. Thus, dysfunction of the KLK-cascade, associated with other proteases, was proposed to regulate cancer progression (Dorn et al., 2014). Because of the broad spectrum of KLK11 regarding hydrolysis activation, it is tempting to speculate that KLK11 has a cascade-initiating potential in ovarian cancer.

Notably, KLKs participate in degradation- and remodelling-proteolytic pathways in tumor extracellular matrix (ECM) by interacting with uPA and/or MMPs (Borgoño and Diamandis, 2004). In addition, KLKs are emerging as key molecules for different signalling pathways. For example, it is well known that the classical tissue kallikrein (KLK1) cleaves kininogen to release kinin (Picard et al., 2005), which might affect angiogenesis and immune response in tumors. Accumulating evidence shows that protease-activated receptors (PARs), known as members of the G-protein-coupled receptor superfamily, are activated by many KLKs (e.g. KLK5, 6, and 14) through cleavage of the extracellular domain, resulting in the presentation of the tethered ligand of the PARs (Oikonomopoulou et al., 2006). Via this process, KLKs are able to regulate

cell migration, tumor metastasis and invasion by a variety of G-protein-coupled substrates. Interestingly, Paliouras and Diamandis (2008) reported a parallel expression pattern of KLK3 and KLK11 in prostate cancer. In this model, KLK3 (PSA) and KLK11 were both positively regulated by signalling pathways of RAS/MEK/ERK and PI3K/AKT. Thus, in prostate cancer, expression of KLK11 and KLK3 seems to be coordinately regulated, which may indicate that both KLKs are involved in prostate cancer progression (Sharma et al., 2002; DeGraffenried et al., 2004). Although no clear evidence there is yet, it is interesting to hypothesize that KLK11 regulates ovarian/breast cancer progression via some important signalling pathways as well.

Interestingly, the present study shows that higher KLK11 mRNA expression reflects poor prognosis in triple-negative breast cancer which is opposite to its prognostic value in high-grade serous ovarian cancer. There is yet no clear explanation about the exact tumor biological role of KLK11 in these tumors. However, it is reasonable to hypothesize that there are different KLK11 substrates in different tumors. Currently, there are indications that KLKs not only act within complex protein networks but target also a number of possible tumor-activating and/or -suppressing signalling pathways. Moreover, it may be important to analyze whether KLK11 is present in active forms in different tumor types. To date, most of the mechanism-related analyses are derived from studies *in vitro*. It remains important to ensure how these mechanism actually operate *in vivo*. Thus, identification of definite endogenous substrates and functional pathways *in vivo*, and once again, analysis of homogeneous cancer subtypes are required to verify a causative link of KLK11 expression with its prognostic value in cancers.

Taken together, it is important to note that cancer subtypes substantially differ with regard to molecular signatures and progression behaviors. Therefore, it is essential to identify and analyze specific subpopulations of ovarian and breast cancer when examining the clinical relevance of KLK11 and KLK15. Furthermore, in the context of complex networks, KLK11/15 might interact with various stimulators and/or suppressors to achieve the physiological and/or pathological regulation. Thus, within

the efforts to regulate KLK11/15, (i) to enhance their tumor-suppressing and/or (ii) to prevent their tumor-supporting roles, it could be a beneficial strategy to figure out their tissue-specific regulators and substrates. In the present study, we found a strong association of elevated KLK11 levels with both favorable OS and PFS in advanced high-grade serous ovarian cancer. It is tempting to speculate that KLK11 has an inhibitory role in advanced high-grade serous ovarian cancer progression, but the biological details are not yet clarified. Although it is not obvious so far to postulate KLK11 as a pharmaceutical target, KLK11 expression might prove as a promising candidate for adjustment and individualization of treatment and to save patients from unnecessary invasive therapy in different types of cancer.

6. Summary

Previous studies have reported that most members of kallikrein-related peptidases are involved in regulation of various tumor-associated processes. In several studies, KLK11 and KLK15 showed potential as prognostic biomarkers for ovarian cancer. However, these studies displayed controversial results analyzing rather heterogeneous patient cohorts including different ovarian cancer subgroups. In the first part of the present study, we used a homogeneous patient cohort encompassing 136 patients afflicted with advanced high-grade serous ovarian cancer (FIGO stage III/IV) and evaluated mRNA expression levels of KLK11 and KLK15 in tumor tissue by quantitative PCR. Most samples displayed a robust expression level of KLK11 mRNA, whereas KLK15 mRNA expression level was low in general. No significant associations of KLK11 and 15 mRNA expression with clinical parameters were found. In univariate Cox regression analyses, higher KLK11 mRNA levels were significantly associated with prolonged OS (HR = 0.53, $p = 0.021$) and PFS (HR = 0.49, $p = 0.008$). KLK15 mRNA levels displayed a trend towards significance in OS (HR = 0.55, $p = 0.060$). In multivariate Cox analyses, higher KLK11 mRNA values, apart from residual tumor mass, remained as an independence favorable predictive marker for both OS (HR = 0.40, $p = 0.007$) and PFS (HR = 0.47, $p = 0.015$). Elevated KLK15 mRNA levels turned out to be significantly associated with longer OS (HR = 0.46, $p = 0.025$) in multivariate analysis.

In the second part of this study, we established immunohistochemical assays for analyzing KLK11 protein levels in ovarian cancer tissues. For this, a specific polyclonal rabbit antibody directed to KLK11 (Abcam ab131038) was used. By adjusting several parameters, an optimised immunohistochemical protocol was established. 153 samples of patients afflicted with advanced high-grade serous ovarian cancer (FIGO III/IV), present on tissue microarrays (TMA), were analyzed. For evaluation of KLK11 immunoreactivity, a digital semi-quantitative immunoreactive score (IRS) was established. This scoring significantly correlated with manual scoring of the TMAs (Spearman, R = 0.594, $p < 0.001$). A robust KLK11 protein expression was observed in

over 50% of the cases. No significant associations of clinical parameters with KLK11 protein expression were found. In univariate Cox regression analysis, higher KLK11 protein levels were significantly associated with prolonged OS (HR = 0.56, $p = 0.025$). In multivariate Cox analysis, higher KLK11 protein values again significantly predict better OS (HR = 0.55, $p = 0.031$).

Because of the predictive value of KLK11 in ovarian cancer, in the third part of this study, we assessed KLK11 mRNA expression levels in breast tumor tissue by quantitative PCR. We selected a homogeneous patient cohort encompassing 108 patients afflicted with triple-negative breast cancer. A stochastically selected patient cohort encompassing 60 hormone-receptor positive breast cancer patients was analyzed as well. In triple-negative breast cancer, most samples display a rather low KLK11 mRNA expression. No significant differences of KLK11 mRNA levels were found between triple-negative and hormone-receptor positive cases. Furthermore, in TNBC, no significant associations of clinical parameters with KLK11 mRNA expression were found. In univariate Cox regression analysis, higher KLK11 mRNA values showed a trend towards shortened 15-years OS (HR = 1.95, $p = 0.052$). When the prognostic value for OS was examined by another type of univariate analysis, Kaplan-Meier survival analysis, a significant result ($p = 0.047$) was obtained. In multivariate Cox analysis, higher KLK11 mRNA values turned out to be significantly associated with shorter 15-years OS (HR = 2.02, $p = 0.044$).

In conclusion, elevated KLK11 values, both mRNA and protein, can be considered as independent favorable prognostic biomarkers in advanced high-grade serous ovarian cancer patients (FIGO III/IV). To a lesser extent, elevated KLK15 mRNA levels are linked with prolonged OS in high-grade serous ovarian cancer patients. Higher KLK11 mRNA levels are significantly associated with worse 15-years OS in triple-negative breast cancer, indicating that the substrates of KLK11 present in advanced high-grade serous ovarian and triple-negative breast cancer may differ.

7. Appendix

7.1 FIGO stage of ovarian cancer

FIGO stage			Tumor description
I		T1, N0, M0	Only in the ovary/ ovaries or fallopian tube(s); No spread to nearby lymph nodes or to distant sites
	IA	T1a, N0, M0	Confined to the inside of one ovary/one fallopian tube; No cancer on the outer surfaces; No cancer cells in ascites or washings from the abdomen/pelvis
	IB	T1b, N0, M0	In both ovaries/fallopian tubes; No cancer on their surfaces; No cancer cells in ascites or washings from the abdomen/pelvis
	IC	T1c, N0, M0	In one or both ovaries or fallopian tubes; Any of the following present: • Broken of tumor capsule during surgery; • On surface of ovaries/fallopian tubes, or ruptured capsule before surgery; • Cancer cells in ascites or washings from the abdomen/pelvis
II		T2, N0, M0	In one or both ovaries or fallopian tubes; Spread to other pelvic organs or primary peritoneal cancer; No spread to nearby lymph nodes or to distant sites
	IIA	T2a, N0, M0	Spread to uterus or fallopian tubes, or ovaries
	IIB	T2b, N0, M0	On outer surface or grown into nearby pelvic organs: bladder, sigmoid colon, or rectum

FIGO stage			Tumor description
III		M0	In one or both ovaries/fallopian tubes, or primary peritoneal cancer; No spread to distant sites
	IIIA1	T1/T2, N1, M0	Possible spread to nearby pelvis organs; Spread to pelvic and/or para-aortic lymph nodes only
	IIIA2	T3a, N0/N1, M0	Spread to organs outside the pelvis; No visible cancer in abdomen during surgery; Tiny deposits of cancer found in lining of abdomen in lab
	IIIB	T3b, N0/N1, M0	Spread to organs outside the pelvis; Visible deposits of cancer ≤ 2 cm
	IIIC	T3c, N0/N1, M0	Spread to organs outside the pelvis; Deposits of cancer > 2 cm, may on liver/spleen capsule; May spread to retroperitoneal lymph nodes; No spread to inside of liver/spleen
IV		M1	With distant metastasis
	IVA	any T, any N, M1a	Malignant pleural effusion; No spread to other areas such as: liver, spleen, intestine, or lymph nodes outside abdomen
	IVB	any T, any N, M1b	Spread to inside of liver/spleen; Spread to lymph nodes other than retroperitoneal lymph nodes, and/or to other organs/tissues outside peritoneal cavity such as: lungs and bones

7.2 Standard dilution serial curves of KLK11 and KLK15

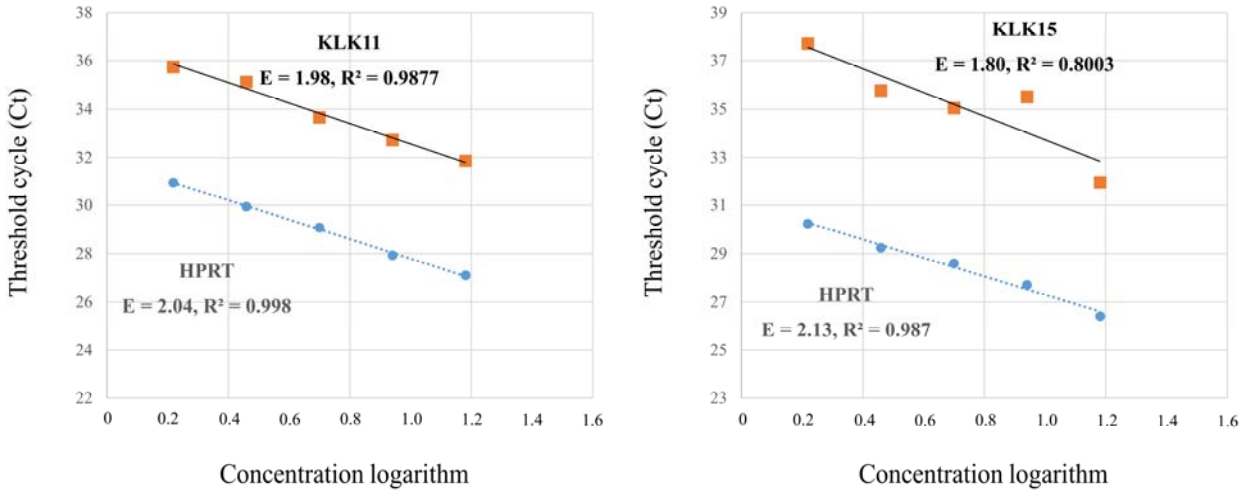

Figure 15. Standard dilution serial curves comparing KLK11 to HPRT, and KLK15 to HPRT, show sufficient mRNA amplification efficiencies.

The mRNA were extracted from OV-KLK11 and OV-KLK15 cell lines. A 2-fold dilution series including 5 concentrations (DNA0-4, range 30-1.875 ng) were prepared for KLK11, KLK15, and housekeeping gene HPRT, respectively. The standard dilution curves comparing KLK11 to HPRT (left) and KLK15 to HPRT (right) were established using qPCR and were depicted by linear regression analysis (for details see **Materials and Methods**). E: efficiency; R^2: Linear regression analysis; 100% efficiency corresponds to an E-value of 2.

7.3 Correlation of KLK11 mRNA expression levels in triple-negative and hormone-receptor positive breast cancer patients

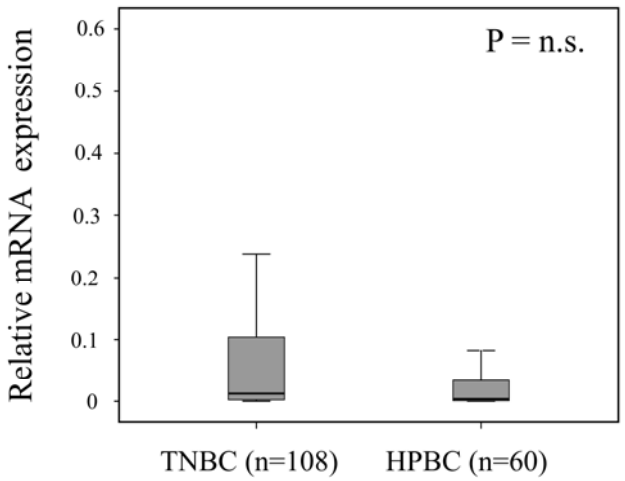

Figure 16. KLK11 mRNA expression levels in triple-negative breast tumor tissues are not associated with those in hormone-receptor positive breast tumors.

We stochastically selected 60 patients afflicted with hormone-receptor positive breast cancer (HPBC). KLK11 mRNA levels in tumor tissues were assessed by qPCR. Independent t test, $p < 0.05$ is considered as statistically significant.

8. Abbreviations

A	area
Ab	antibody
AKT	protein kinase B
BLBC	basal-like breast cancers
BPH	benign prostatic hyperplasia
BRCA1	breast cancer gene 1
CA125	cancer antigen 125
cDNA	complementary deoxyribonucleic acid
CI	confidence interval
CK5/6	cytokeratin 5/6
Ct	cycle threshold
DAB	diaminobenzidine
DCIS	ductal carcinoma *in situ*
DNA	desoxyriunicleic acid
dNTP	deoxyribonucleoside triphosphate
E	efficiency
ECL	enhanced chemilumescent
ECM	tumor extracellular matrix
EGFR	epidermal growth factor receptor
ELISA	enzyme-linked immunosorbent assay
EP	error propagation
ER	estrogen receptor
ERK	extracellular signal-regulated kinases
FIGO	international federation of gynecology and obstetrics
FOLFOX4	chemotherapy regimen made up of drugs: FOL(folinic acid), F(fluorouracil, 5-FU), and OX(oxaliplatin)
GSE	Genomic Spatial Event

H&E	hematoxylin and eosin
HER2	human epidermal growth factor receptor 2
HGSOC	high-grade serous ovarian cancer
HPBC	hormone-receptor positive breast cancer
HPRT	hypoxanthine phosphoribosyltransferase
HR	homologous recombination
HR	hazard ratio
HRP	horseradish peroxidase
IHC	immunohistochemistry
InD	integrated gray density
IRS	immunoreactive score
kDa	kilo dalton
KLK	kallikrein-related peptidases
KM	Kaplan-Meier
ln	natural logarithm
MAPK	mitogen-activated protein kinases
MEK	mitogen-activated protein kinase kinase
MMP	matrix metalloprotease
mTOR	mammalian target of rapamycin
NS	netherton syndrome
NSCLC	non-small cell lung cancer
OD	optical density
OS	overall survival
PAA	polyacrylamide
PAGE	polyacrylamide gel electrophoresis
PAI-1	plasminogen activator inhibitor-1
PARP	poly ADP-ribose polymerase
PARs	protease-activated receptor
PD-1	programmed death 1

PD-L1	programmed death-ligand 1
PFS	progression-free survival
PI3K	phosphoinositide 3-kinase
RGB	red, green, blue
PR	progesterone receptor
PSA	prostate-specific antigen
PVDF	polyvinylidene difluoride
Q	quartile
qPCR	quantitative real-time polymerase chain reaction
RNA	ribonucleic acid
RT	reverse transcription
RT	room temperature
SCCE	stratum corneum chymotryptic enzyme
SCTE	stratum corneum tryptic enzyme
SPINK5	serine protease inhibitor Kazal-type 5
STDEV	standard deviation
TCGA	Cancer Genome Atlas
TMA	tumor tissue microarrays
TNBC	triple-negative breast cancer
TNM	TNM (primary tumor, lymph nodes, distant metastasis) classification of malignant tumors
TVUS	transvaginal ultrasound
uPA	urokinase-type plasminogen
UPL	universal probe library
VEGF	vascular endothelial growth factor
WB	western blotting
1,25D	1 alpha, 25-dihydroxyvitamin D3

9. References

Ahmed N, Dorn J, Napieralski R, Drecoll E, Kotzsch M, Goettig P, Zein E, Avril S, Kiechle M, Diamandis EP, Schmitt M, Magdolen V. Clinical relevance of kallikrein-related peptidase 6 (KLK6) and 8 (KLK8) mRNA expression in advanced serous ovarian cancer. Biol Chem. 2016, 397(12): 1265-76.

Anderson WF, Rosenberg PS, Prat A, Perou CM, Sherman ME. How many etiological subtypes of breast cancer: two, three, four, or more? J Natl Cancer Inst. 2014, 106(8) pii: dju165.

Au-Yeung G, Lang F, Azar WJ, Mitchell C, Jarman KE, Lackovic K, Aziz D, Cullinane C, Pearson RB, Mileshkin L, Rischin D, Karst AM, Drapkin R, Etemadmoghadam D, Bowtell DDL. Selective targeting of Cyclin E1-amplified high-grade serous ovarian cancer by Cyclin-dependent kinase 2 and AKT inhibition. Clin Cancer Res. 2017, 23(7): 1862-74.

Bell D, Berchuck A, Birrer M, Chien J, Cramer DW, Dao F, Dhir R, DiSaia P, Gabra H, Glenn P, Godwin AK, Gross J, Hartmann L, Huang M, Huntsman DG, Iacocca M, Imielinski M, Kalloger S, Karlan BY, Levine DA, Mills GB, Morrison C, Mutch D, Olvera N, Orsulic S, Park K, Petrelli N, Rabeno B, Rader JS, Sikic BI, Smith-McCune K, Sood AK, Bowtell D, Penny R, Testa JR, Chang K, Dinh HH, Drummond JA, Fowler G, Gunaratne P, Hawes AC, Kovar CL, Lewis LR, Morgan MB, Newsham IF, Santibanez J, Reid JG, Trevino LR, Wu YQ, Wang M, Muzny DM, Wheeler DA, Gibbs RA, Getz G, Lawrence MS, Cibulskis K, Sivachenko AY, Sougnez C, Voet D, Wilkinson J, Bloom T, Ardlie K, Fennell T, Baldwin J, Gabriel S, Lander ES, Ding L, Fulton RS, Koboldt DC, McLellan MD, Wylie T, Walker J, O'Laughlin M, Dooling DJ, Fulton L, Abbott R, Dees ND, Zhang Q, Kandoth C, Wendl M, Schierding W, Shen D, Harris CC, Schmidt H, Kalicki J, Delehaunty KD, Fronick CC, Demeter R, Cook L, Wallis JW, Lin L, Magrini VJ, Hodges JS, Eldred JM, Smith SM, Pohl CS, Vandin F,

Raphael BJ, Weinstock GM, Mardis R, Wilson RK, Meyerson M, Winckler W, Getz G, Verhaak RGW, Carter SL, Mermel CH, Saksena G, Nguyen H, Onofrio RC, Lawrence MS, Hubbard D, Gupta S, Crenshaw A, Ramos AH, Ardlie K, Chin L, Protopopov A, Zhang JH, Kim TM, Perna I, Xiao Y, Zhang H, Ren G, Sathiamoorthy N, Park RW, Lee E, Park PJ, Kucherlapati R, Absher DM, Waite L, Sherlock G, Brooks JD, Li JZ, Xu J, Myers RM, Laird PW, Cope L, Herman JG, Shen H, Weisenberger DJ, Noushmehr H, Pan F, Triche T, Berman BP, Van den Berg DJ, Buckley J, Baylin SB, Spellman PT, Purdom E, Neuvial P, Bengtsson H, Jakkula LR, Durinck S, Han J, Dorton S, Marr H, Choi YG, Wang V, Wang NJ, Ngai J, Conboy JG, Parvin B, Feiler HS, Speed TP, Gray JW, Levine DA, Socci ND, Liang Y, Taylor BS, Schultz N, Borsu L, Lash AE, Brennan C, Viale A, Sander C, Ladanyi M, Hoadley KA, Meng S, Du Y, Shi Y, Li L, Turman YJ, Zang D, Helms EB, Balu S, Zhou X, Wu J, Topal MD, Hayes DN, Perou CM, Getz G, Voet D, Saksena G, Zhang JNH, Zhang H, Wu CJ, Shukla S, Cibulskis K, Lawrence MS, Sivachenko A, Jing R, Park RW, Liu Y, Park PJ, Noble M, Chin L, Carter H, Kim D, Karchin R, Spellman PT, Purdom E, Neuvial P, Bengtsson H, Durinck S, Han J, Korkola JE, Heiser LM, Cho RJ, Hu Z, Parvin B, Speed TP, Gray JW, Schultz N, Cerami E, Taylor BS, Olshen A, Reva B, Antipin Y, Shen R, Mankoo P, Sheridan R, Ciriello G, Chang WK, Bernanke JA, Borsu L, Levine DA, Ladanyi M, Sander C, Haussler D, Benz CC, Stuart JM, Benz SC, Sanborn JZ, Vaske CJ, Zhu J, Szeto C, Scott GK, Yau C, Hoadley KA, Du Y, Balu S, Hayes DN, Perou CM, Wilkerson MD, Zhang N, Akbani R, Baggerly KA, Yung WK, Mills GB, Weinstein JN, Penny R, Shelton T, Grimm D, Hatfield M, Morris S, Yena P, Rhodes P, Sherman M, Paulauskis J, Millis S, Kahn A, Greene JM, Sfeir R, Jensen MA, Chen J, Whitmore J, Alonso S, Jordan J, Chu A, Zhang JH, Barker A, Compton C, Eley G, Ferguson M, Fielding P, Gerhard DS, Myles R, Schaefer C, Shaw KRM, Vaught J, Vockley JB, Good PJ, Guyer MS, Ozenberger B, Peterson J, Thomson E. Cancer Genome Atlas Research Network. Integrated genomic analyses of ovarian carcinoma. Nature. 2011, 474(7353): 609-15.

Borgoño CA, Diamandis EP. The emerging roles of human tissue kallikreins in cancer. Nat Rev Cancer. 2004, 4(11): 876-90.

Borgoño CA, Fracchioli S, Yousef GM, Rigault de la Longrais IA, Luo LY, Soosaipillai A, Puopolo M, Grass L, Scorilas A, Diamandis EP, Katsaros D. Favorable prognostic value of tissue human kallikrein 11 (hK11) in patients with ovarian carcinoma. Int J Cancer. 2003, 106(4): 605-10.

Bowtell DD, Bohm S, Ahmed AA, Aspuria PJ, Bast RC, Jr., Beral V, Berek JS, Birrer MJ, Blagden S, Bookman MA, Brenton JD, Chiappinelli KB, Martins FC, Coukos G, Drapkin R, Edmondson R, Fotopoulou C, Gabra H, Galon J, Gourley C, Heong V, Huntsman DG, Iwanicki M, Karlan BY, Kaye A, Lengyel E, Levine DA, Lu KH, McNeish IA, Menon U, Narod SA, Nelson BH, Nephew KP, Pharoah P, Powell DJ, Jr., Ramos P, Romero IL, Scott CL, Sood AK, Stronach EA, Balkwill FR. Rethinking ovarian cancer II: reducing mortality from high-grade serous ovarian cancer. Nature Rev Cancer. 2015, 15(11): 668-79.

Brattsand M, Stefansson K, Lundh C, Haasum Y, Egelrud T. A proteolytic cascade of kallikreins in the stratum corneum. J Invest Dermatol. 2005, 124(1): 198-203.

Bustin SA, Nolan T. Analysis of mRNA expression by real-time PCR. Real-Time Pcr: Advanced Technologies and Applications. 2013. 51-88.

Buys SS, Partridge E, Black A, Johnson CC, Lamerato L, Isaacs C, Reding DJ, Greenlee RT, Yokochi LA, Kessel B, Crawford ED, Church TR, Andriole GL, Weissfeld JL, Fouad MN, Chia D, O'Brien B, Ragard LR, Clapp JD, Rathmell JM, Riley TL, Hartge P, Pinsky PF, Zhu CS, Izmirlian G, Kramer BS, Miller AB, Xu JL, Prorok PC, Gohagan JK, Berg CD. Effect of screening on ovarian cancer mortality: the Prostate, Lung, Colorectal and Ovarian (PLCO) Cancer Screening Randomized Controlled Trial. JAMA. 2011, 305(22): 2295-303.

Beaufort N, Plaza K, Utzschneider D, Schwarz A, Burkhart JM, Creutzburg S, Debela

M, Schmitt M, Ries C, Magdolen V. Interdependence of kallikrein-related peptidases in proteolytic networks. Biol Chem. 2010, 391(5): 581-7.

Biesterfeld S, Veuskens U, Schmitz FJ, AmoTakyi B, Böcking A. Interobserver reproducibility of immunocytochemical estrogen- and progesterone receptor status assessment in breast cancer. Anticancer Res. 1996, 16: 2497-500.

Cardoso F, Costa A, Norton L, Senkus E, Aapro M, Andre F, Barrios CH, Bergh J, Biganzoli L, Blackwell KL, Cardoso MJ, Cufer T, El Saghir N, Fallowfield L, Fenech D, Francis P, Gelmon K, Giordano SH, Gligorov J, Goldhirsch A, Harbeck N, Houssami N, Hudis C, Kaufman B, Krop I, Kyriakides S, Lin UN, Mayer M, Merjaver SD, Nordstrom EB, Pagani O, Partridge A, Penault-Llorca F, Piccart MJ, Rugo H, Sledge G, Thomssen C, Van't Veer L, Vorobiof D, Vrieling C, West N, Xu B, Winer E. ESO-ESMO 2nd international consensus guidelines for advanced breast cancer (ABC2). Breast. 2014, 23(5): 489-502.

Carlson RW, Allred DC, Anderson BO, Burstein HJ, Carter WB, Edge SB, Erban JK, Farrar WB, Goldstein LJ, Gradishar WJ, Hayes DF, Hudis CA, Jahanzeb M, Kiel K, Ljung BM, Marcom PK, Mayer IA, McCormick B, Nabell LM, Pierce LJ, Reed EC, Smith ML, Somlo G, Theriault RL, Topham NS, Ward JH, Winer EP, Wolff AC, NCCN Breast Cancer Clinical Practice Guidelines Panel. Breast cancer. Clinical practice guidelines in oncology. J Natl Compr Canc Netw. 2009, 7(2): 122-92.

Cassim B, Mody G, Bhoola KD. Kallikrein cascade and cytokines in inflamed joints. Pharmacol Ther. 2002, 94(1-2): 1-34.

Cho KR, Shih leM. Ovarian cancer. Annu Rev Pathol. 2009, 4: 287-313.

Ciriello G, Miller ML, Aksoy BA, Senbabaoglu Y, Schultz N, Sander C. Emerging landscape of oncogenic signatures across human cancers. Nature Genet. 2013, 45(10):

1127-33.

Clarkson RW, Boland MP, Kritikou EA, Lee JM, Freeman TC, Tiffen PG, Watson CJ. The genes induced by signal transducer and activators of transcription (STAT) 3 and STAT5 in mammary epithelial cells define the roles of these STATs in mammary development. Mol Endocrino. 2006, 20(3): 675-85.

Commoner B, Lipkin D. The application of the Beer-Lambert law to optically anisotropic systems. Science.1949, 110(2845): 41-3.

Costa RLB, Han HS, Gradishar WJ. Targeting the PI3K/AKT/mTOR pathway in triple-negative breast cancer: a review. Breast Cancer Res Treat. 2018, 169(3): 397-406.

Costa R, Shah AN, Santa-Maria CA, Cruz MR, Mahalingam D, Carneiro BA, Chae YK, Cristofanilli M, Gradishar WJ, Giles FJ. Targeting epidermal growth factor receptor in triple negative breast cancer: new discoveries and practical insights for drug development. Cancer Treat Rev. 2017, 53: 111-9.

Curigliano G, Burstein HJ, Winer EP, Gnant M, Dubsky P, Loibl S, Colleoni M, Regan MM, Piccart-Gebhart M, Senn HJ, Thurlimann B, St Gallen Int Expert C. De-escalating and escalating treatments for early-stage breast cancer: the St. Gallen International Expert Consensus Conference on the Primary Therapy of Early Breast Cancer 2017. Ann Oncol. 2017, 28(8): 1700-12.

DeGraffenried LA, Fulcher L, Friedrichs WE, Grunwald V, Ray RB, Hidalgo M. Reduced PTEN expression in breast cancer cells confers susceptibility to inhibitors of the PI3 kinase/Akt pathway. Ann Oncol. 2004, 15(10): 1510-6.

Denkert C, Liedtke C, Tutt A, von Minckwitz G. Molecular alterations in triple-negative breast cancer-the road to new treatment strategies. Lancet. 2017, 389 (10087): 2430-42.

Dettmar L, Ahmed N, Kotzsch M, Diersch S, Napieralski R, Darmoul D, Schmitt M, Weichert W, Kiechle M, Dorn J, Magdolen V. Advanced high-grade serous ovarian cancer: inverse association of KLK13 and KLK14 mRNA levels in tumor tissue and patients' prognosis. J Cancer Res Clin Oncol. 2018, 144(6): 1109-18.

DeSantis C, Ma J, Bryan L, Jemal A. Breast cancer statistics, 2013. CA Cancer J Clin. 2014, 64(1): 52-62.

de Veer SJ, Furio L, Swedberg JE, Munro CA, Brattsand M, Clements JA, Hovnanian A, Harris JM. Selective substrates and inhibitors for kallikrein-related peptidase 7 (KLK7) shed light on KLK proteolytic activity in the stratum corneum. J Invest Dermatol. 2017, 137(2): 430-9.

Diamandis EP. New diagnostic applications and physiological functions of prostate specific antigen. Scand J Clin Lab Invest Suppl. 1995, 221: 105-12.

Diamandis EP, Borgoño CA, Scorilas A, Harbeck N, Dorn J, Schmitt M. Human kallikrein 11: an indicator of favorable prognosis in ovarian cancer patients. Clin Biochem. 2004, 37(9): 823-9.

Dillon JL, Mockus SM, Ananda G, Spotlow V, Wells WA, Tsongalis GJ, Marotti JD. Somatic gene mutation analysis of triple negative breast cancers. Breast. 2016, 29: 202-7.

Dorn J, Beaufort N, Schmitt M, Diamandis EP, Goettig P, Magdolen V. Function and clinical relevance of kallikrein-related peptidases and other serine proteases in gynecological cancers. Crit Rev Clin Lab Sci. 2014, 51(2): 63-84.

Dorn J, Bronger H, Kates R, Slotta-Huspenina J, Schmalfeldt B, Kiechle M, Diamandis

EP, Soosaipillai A, Schmitt M, Harbeck N. OVSCORE - a validated score to identify ovarian cancer patients not suitable for primary surgery. Oncol Lett. 2015, 9(1): 418-24.

Dorn J, Gkazepis A, Kotzsch M, Kremer M, Propping C, Mayer K, Mengele K, Diamandis EP, Kiechle M, Magdolen V, Schmitt M. Clinical value of protein expression of kallikrein-related peptidase 7 (KLK7) in ovarian cancer. Biol Chem. 2014, 395(1): 95-107.

Dorn J, Yassouridis A, Walch A, Diamandis EP, Schmitt M, Kiechle M, Wang P, Drecoll E, Schmalfeldt B, Loessner D, Kotzsch M, Magdolen V. Assessment of kallikrein-related peptidase 5 (KLK5) protein expression in tumor tissue of advanced ovarian cancer patients by immunohistochemistry and ELISA: correlation with clinical outcome. Am J Cancer Res. 2016, 6(1): 61-70.

Drapkin R, Stronach E, Gabra H, Brown R, Jewell A, Nagaraj SH, Markham E, Wilson PJ, Ellul J, McNally O, Doyle MA, Vedururu R, Stewart C, Lengyel E, Pearson JV, Waddell N, deFazio A, Grimmond SM, Bowtell DD. Whole-genome characterization of chemoresistant ovarian cancer. Nature. 2015, 521(7553): 489-94.

Elsawaf Z, Sinn HP. Triple-negative breast cancer: clinical and histological correlations. Breast care. 2011, 6(4): 273-8.

Fan J, Tea MK, Yang C, Ma L, Meng QH, Hu TY, Singer CF, Ferrari M. Profiling of cross-functional peptidases regulated circulating peptides in BRCA1 mutant breast cancer. J Proteome Res. 2016, 15(5): 1534-45.

Fleshner K, Carlsson SV, Roobol MJ. The effect of the USPSTF PSA screening recommendation on prostate cancer incidence patterns in the USA. Nat Rev Urol. 2017, 14(1): 26-37.

Foulkes WD, Smith IE, Reis-Filho JS. Triple-negative breast cancer. New Engl J Med. 2010, 363(20): 1938-48.

Geenen JJJ, Linn SC, Beijnen JH, Schellens JHM. PARP inhibitors in the treatment of triple-negative breast cancer. Clin Pharmacokinet. 2018, 57(4): 427-37.

Gelmon KA, Tischkowitz M, Mackay H, Swenerton K, Robidoux A, Tonkin K, Hirte H, Huntsman D, Clemons M, Gilks B, Yerushalmi R, Macpherson E, Carmichael J, Oza A. Olaparib in patients with recurrent high-grade serous or poorly differentiated ovarian carcinoma or triple-negative breast cancer: a phase 2, multicentre, open-label, non-randomised study. Lancet Oncol. 2011, 12(9): 852-61.

Goettig P, Magdolen V, Brandstetter H. Natural and synthetic inhibitors of kallikrein-related peptidases (KLKs). Biochimie. 2010, 92(11): 1546-67.

Goff BA, Mandel LS, Melancon CH, Muntz HG. Frequency of symptoms of ovarian cancer in women presenting to primary care clinics. JAMA. 2004, 291(22): 2705-12.

Gradishar WJ, Anderson BO, Balassanian R, Blair SL, Burstein HJ, Cyr A, Elias AD, Farrar WB, Forero A, Giordano SH, Goetz M, Goldstein LJ, Hudis CA, Isakoff SJ, Marcom PK, Mayer IA, McCormick B, Moran M, Patel SA, Pierce LJ, Reed EC, Salerno KE, Schwartzberg LS, Smith KL, Smith ML, Soliman H, Somlo G, Telli M, Ward JH, Shead DA, Kumar R. Breast Cancer Version 2.2015. J Natl Compr Canc Netw. 2015, 13(4): 448-75.

Gyorffy B, Lanczky A, Szallasi Z. Implementing an online tool for genome-wide validation of survival-associated biomarkers in ovarian-cancer using microarray data from 1287 patients. Endocr Relat Cancer. 2012, 19(2): 197-208.

Harbeck N, Gluz O. Neoadjuvant therapy for triple negative and HER2-positive early breast cancer. Breast. 2017, 34 Suppl 1: S99-s103.

Harbeck N, Gnant M. Breast cancer. Lancet. 2017, 389(10074): 1134-50.

Haritos C, Michaelidou K, Mavridis K, Missitzis I, Ardavanis A, Griniatsos J, Scorilas A. Kallikrein-related peptidase 6 (KLK6) expression differentiates tumor subtypes and predicts clinical outcome in breast cancer patients. Clin Exp Med. 2018, 18(2): 203-13.

Hida AI, Sagara Y, Yotsumoto D, Kanemitsu S, Kawano J, Baba S, Rai Y, Oshiro Y, Aogi K, Sagara Y, Ohi Y. Prognostic and predictive impacts of tumor-infiltrating lymphocytes differ between triple-negative and HER2-positive breast cancers treated with standard systemic therapies. Breast Cancer Res Treat. 2016, 158(1): 1-9.

Holschneider CH, Berek JS. Ovarian cancer: epidemiology, biology, and prognostic factors. Semin Surg Oncol. 2000, 19(1): 3-10.

Howitt BE, Hanamornroongruang S, Lin DI, Conner JE, Schulte S, Horowitz N, Crum CP, Meserve EE. Evidence for a dualistic model of high-grade serous carcinoma: BRCA mutation status, histology, and tubal intraepithelial carcinoma. Am J Surg Pathol. 2015, 39(3): 287-93.

Hu XC, Huang W, Fan MH. Emerging therapies for breast cancer. J Hematol Oncol. 2017, 10(1): 98.

Ibrahim YH, Garcia-Garcia C, Serra V, He L, Torres-Lockhart K, Prat A, Anton P, Cozar P, Guzman M, Grueso J, Rodriguez O, Calvo MT, Aura C, Diez O, Rubio IT, Perez J, Rodon J, Cortes J, Ellisen LW, Scaltriti M, Baselga J. PI3K inhibition impairs BRCA1/2 expression and sensitizes BRCA-proficient triple-negative breast cancer to PARP inhibition. Cancer Discov. 2012, 2(11): 1036-47.

Ishikawa Y, Horiguchi J, Toya H, Nakajima H, Hayashi M, Tagaya N, Takeyoshi I, Oyama T. Triple-negative breast cancer: histological subtypes and immunohistochemical and clinicopathological features. Cancer Sci. 2011, 102(3): 656-62.

Jamaspishvili T, Scorilas A, Kral M, Khomeriki I, Kurfurstova D, Kolar Z, Bouchal J. Immunohistochemical localization and analysis of kallikrein-related peptidase 7 and 11 expression in paired cancer and benign foci in prostate cancer patients. Neoplasma. 2011, 58(4): 298-303.

Jayson GC, Kohn EC, Kitchener HC, Ledermann JA. Ovarian cancer. Lancet. 2014, 384(9951): 1376-88.

Kapadia C, Ghosh MC, Grass L, Diamandis EP. Human kallikrein 13 involvement in extracellular matrix degradation. Biochem Biophys Res Commun. 2004, 323(3): 1084-90.

Karnezis AN, Cho KR, Gilks CB, Pearce CL, Huntsman DG. The disparate origins of ovarian cancers: pathogenesis and prevention strategies. Nat Rev Cancer. 2017, 17(1): 65-74.

Kasparek P, Ileninova Z, Zbodakova O, Kanchev I, Benada O, Chalupsky K, Brattsand M, Beck IM, Sedlacek R. KLK5 and KLK7 ablation fully rescues lethality of Netherton syndrome-like phenotype. Plos Genet. 2017, 13(1).

King MC, Marks JH, Mandell JB. Breast and ovarian cancer risks due to inherited mutations in BRCA1 and BRCA2. Science. 2003, 302(5645): 643-6.

Kolin DL, Sy K, Rotondo F, Bassily MN, Kovacs K, Brezden-Masley C, Streutker CJ, Yousef GM. Prognostic significance of human tissue kallikrein-related peptidases 11

and 15 in gastric cancer. Tumour Biol. 2016, 37(1): 437-46.

Komatsu N, Saijoh K, Kuk C, Liu AC, Khan S, Shirasaki F, Takehara K, Diamandis EP. Human tissue kallikrein expression in the stratum corneum and serum of atopic dermatitis patients. Exp Dermatol. 2007a, 16(6): 513-9.

Komatsu N, Saijoh K, Kuk C, Shirasaki F, Takehara K, Diamandis EP. Aberrant human tissue kallikrein levels in the stratum corneum and serum of patients with psoriasis: dependence on phenotype, severity and therapy. Br J Dermatol. 2007b, 156(5): 875-83.

Kuchenbaecker KB, Hopper JL, Barnes DR, Phillips KA, Mooij TM, Roos-Blom MJ, Jervis S, van Leeuwen FE, Milne RL, Andrieu N, Goldgar DE, Terry MB, Rookus MA, Easton DF, Antoniou AC, Consortium BBC. Risks of breast, ovarian, and contralateral breast cancer for BRCA1 and BRCA2 mutation carriers. JAMA. 2017, 317(23): 2402-16.

Kuhn E, Kurman RJ, Vang R, Sehdev AS, Han GM, Soslow R, Wang TL, Shih IM. TP53 mutations in serous tubal intraepithelial carcinoma and concurrent pelvic high-grade serous carcinoma-evidence supporting the clonal relationship of the two lesions. J Pathol. 2012, 226(3): 421-6.

Kurman RJ, Shih IeM. The origin and pathogenesis of epithelial ovarian cancer: a proposed unifying theory. Am J Surg Pathol. 2010, 34(3): 433-43.

Ledermann JA, El-Khouly F. PARP inhibitors in ovarian cancer: Clinical evidence for informed treatment decisions. Br J Cancer. 2015, 113: S10-6.

Lehmann BD, Bauer JA, Chen X, Sanders ME, Chakravarthy AB, Shyr Y, Pietenpol JA. Identification of human triple-negative breast cancer subtypes and preclinical models for selection of targeted therapies. J Clin Invest. 2011, 121(7): 2750-67.

Lehmann BD, Jovanovic B, Chen X, Estrada MV, Johnson KN, Shyr Y, Moses HL, Sanders ME, Pietenpol JA. Refinement of triple-negative breast cancer molecular subtypes: implications for neoadjuvant chemotherapy selection. PLoS One. 2016, 11(6).

Leung F, Bernardini MQ, Brown MD, Zheng Y, Molina R, Bast RC, Jr., Davis G, Serra S, Diamandis EP, Kulasingam V. Validation of a novel biomarker panel for the detection of ovarian cancer. Cancer Epidemiol Biomarkers Prev. 2016, 25(9): 1333-40.

Loessner D, Goettig P, Preis S, Felber J, Bronger H, Clements JA, Dorn J, Magdolen V. Kallikrein-related peptidases represent attractive therapeutic targets for ovarian cancer. Expert Opin Ther Targets. 2018, 22(9): 745-63.

Lu X, Pan J, Li S, Shen S, Chi P, Lin H, Huang Y, Xu Z, Huang S. Establishment of a predictive genetic model for estimating chemotherapy sensitivity of colorectal cancer with synchronous liver metastasis. Cancer Biother Radiopharm. 2013, 28(7): 552-8.

Luo LY, Shan SJ, Elliott MB, Soosaipillai A, Diamandis EP. Purification and characterization of human kallikrein 11, a candidate prostate and ovarian cancer biomarker, from seminal plasma. Clin Cancer Res. 2006, 12(3 Pt 1): 742-50.

Makki J. Diversity of breast carcinoma: histological subtypes and clinical relevance. Clin Med Insights Pathol. 2015, 8: 23-31.

Malhotra GK, Zhao X, Band H, Band V. Histological, molecular and functional subtypes of breast cancers. Cancer Biol Ther. 2010, 10(10): 955-60.

Malvezzi M, Carioli G, Bertuccio P, Rosso T, Boffetta P, Levi F, La Vecchia C, Negri E. European cancer mortality predictions for the year 2016 with focus on leukaemias. Ann Oncol. 2016, 27(4): 725-31.

Mange A, Dimitrakopoulos L, Soosaipillai A, Coopman P, Diamandis EP, Solassol J. An integrated cell line-based discovery strategy identified follistatin and kallikrein 6 as serum biomarker candidates of breast carcinoma. J Proteomics. 2016, 142: 114-21.

Matsuda N, Lim B, Wang XP, Ueno NT. Early clinical development of epidermal growth factor receptor targeted therapy in breast cancer. Expert Opin Investig Drugs. 2017, 26(4): 463-79.

Mavridis K, Stravodimos K, Scorilas A. Quantified KLK15 gene expression levels discriminate prostate cancer from benign tumors and constitute a novel independent predictor of disease progression. Prostate. 2013, 73(11): 1191-201.

McIntosh MW, Liu Y, Drescher C, Urban N, Diamandis EP. Validation and characterization of human kallikrein 11 as a serum marker for diagnosis of ovarian carcinoma. Clin Cancer Res. 2007, 13(15 Pt 1): 4422-8.

Michaelidou K, Ardavanis A, Scorilas A. Clinical relevance of the deregulated kallikrein-related peptidase 8 mRNA expression in breast cancer: a novel independent indicator of disease-free survival. Breast Cancer Res Treat. 2015, 152(2): 323-36.

Mirza MR, Monk BJ, Herrstedt J, Oza AM, Mahner S, Redondo A, Fabbro M, Ledermann JA, Lorusso D, Vergote I, Ben-Baruch NE, Marth C, Madry R, Christensen RD, Berek JS, Dorum A, Tinker AV, du Bois A, Gonzalez-Martin A, Follana P, Benigno B, Rosenberg P, Gilbert L, Rimel BJ, Buscema J, Balser JP, Agarwal S, Matulonis UA. Niraparib maintenance therapy in platinum-sensitive, recurrent ovarian cancer. N Engl J Med. 2016, 75(22): 2154-64.

Mo W, Liu Q, Lin CC, Dai H, Peng Y, Liang Y, Peng G, Meric-Bernstam F, Mills GB, Li K, Lin SY. mTOR inhibitors suppress homologous recombination repair and synergize with PARP inhibitors via regulating SUV39H1 in BRCA-proficient triple-

negative breast cancer. Clin Cancer Res. 2016, 22(7): 1699-712.

Noone AM, Howlader N, Krapcho M, Miller D, Brest A, Yu M, Ruhl J, Tatalovich Z, Mariotto A, Lewis DR, Chen HS, Feuer EJ, Cronin KA. SEER Cancer Statistics Review, 1975-2015, National Cancer Institute. Based on November 2017 SEER data submission, posted to web site, April 2018.

Oikonomopoulou K, Hansen KK, Saifeddine M, Tea I, Blaber M, Blaber SI, Scarisbrick I, Andrade-Gordon P, Cottrell GS, Bunnett NW, Diamandis EP, Hollenberg MD. Proteinase-activated receptors, targets for kallikrein signaling. J Biol Chem. 2006, 281(43): 32095-112.

Ossovskaya V, Wang Y, Budoff A, Xu Q, Lituev A, Potapova O, Vansant G, Monforte J, Daraselia N. Exploring molecular pathways of triple-negative breast cancer. Genes Cancer. 2011, 2(9): 870-9.

Paliouras M, Diamandis EP. Intracellular signaling pathways regulate hormone-dependent kallikrein gene expression. Tumour Biol. 2008, 29(2): 63-75.

Pampalakis GS, otiropoulou G. Tissue kallikrein proteolytic cascade pathways in normal physiology and cancer. Biochim Biophys Acta. 2007, 1776(1): 22-31.

Patch AM, Christie EL, Etemadmoghadam D, Garsed DW, George J, Fereday S, Nones K, Cowin P, Alsop K, Bailey PJ, Kassahn KS, Newell F, Quinn MC, Kazakoff S, Quek K, Wilhelm-Benartzi C, Curry E, Leong HS, Hamilton A, Mileshkin L, Au-Yeung G, Kennedy C, Hung J, Chiew YE, Harnett P, Friedlander M, Quinn M, Pyman J, Cordner S, O'Brien P, Leditschke J, Young G, Strachan K, Waring P, Azar W, Mitchell C, Traficante N, Hendley J, Thorne H, Shackleton M, Miller DK, Arnau GM, Tothill RW, Holloway TP, Semple T, Harliwong I, Nourse C, Nourbakhsh E, Manning S, Idrisoglu S, Bruxner TJ, Christ AN, Poudel B, Holmes O, Anderson M, Leonard C, Lonie A, Hall

N, Wood S, Taylor DF, Xu Q, Fink JL, Waddell N, Perou CM, Sorlie T, Eisen MB, van de Rijn M, Jeffrey SS, Rees CA, Pollack JR, Ross DT, Johnsen H, Akslen LA, Fluge O, Pergamenschikov A, Williams C, Zhu SX, Lonning PE, Borresen-Dale AL, Brown PO, Botstein D. Molecular portraits of human breast tumours. Nature. 2000, 406(6797): 747-52.

Patsis C, Yiotakis I, Scorilas A. Diagnostic and prognostic significance of human kallikrein 11 (KLK11) mRNA expression levels in patients with laryngeal cancer. Clin Biochem. 2012, 45(9): 623-30.

Pavlopoulou A, Pampalakis G, Michalopoulos I, Sotiropoulou G. Evolutionary history of tissue kallikreins. PloS One. 2010, 5(11): e13781.

Perets R, Wyant GA, Muto KW, Bijron JG, Poole BB, Chin KT, Chen JY, Ohman AW, Stepule CD, Kwak S, Karst AM, Hirsch MS, Setlur SR, Crum CP, Dinulescu DM, Drapkin R. Transformation of the fallopian tube secretory epithelium leads to high-grade serous ovarian cancer in Brca;Tp53;Pten models. Cancer cell. 2013, 24(6): 751-65.

Perez EA, Moreno-Aspitia A, Thompson EA, Andorfer CA. Adjuvant therapy of triple negative breast cancer. Breast Cancer Res Treat. 2010, 120(2): 285-91.

Perou CM, Sorlie T, Eisen MB, van de Rijn M, Jeffrey SS, Rees CA, Pollack J R, Ross DT, Johnsen H, Akslen LA, Fluge O, Pergamenschikov A, Williams C, Zhu S X, Lonning PE, Borresen-Dale AL, Brown PO, Botstein D. Molecular portraits of human breast tumours. Nature. 2000, 406, (6797): 747-52.

Pfaffl MW. Quantification strategies in real-time polymerase chain reaction. Quantitative Real-Time Pcr in Applied Microbiology. 2012. 53-61.

Picard N, Van Abel M, Campone C, Seiler M, Bloch-Faure M, Hoenderop JGJ, Loffing J, Meneton P, Bindels RJM, Paillard M, Alhenc-Gelas F, Houillier P. Tissue kallikrein-deficient mice display a defect in renal tubular calcium absorption. J Am Soc Nephrol. 2005, 16(12): 3602-10.

Pinsky PF, Prorok PC, Yu K, Kramer BS, Black A, Gohagan JK, Crawford ED, Grubb RL, Andriole GL. Extended mortality results for prostate cancer screening in the PLCO trial with median follow-up of 15 years. Cancer. 2017, 123(4): 592-9.

Pradeep S, Kim SW, Wu SY, Nishimura M, Chaluvally-Raghavan P, Miyake T, Pecot CV, Kim SJ, Choi HJ, Bischoff FZ, Mayer JA, Huang L, Nick AM, Hall CS, Rodriguez-Aguayo C, Zand B, Dalton HJ, Arumugam T, Lee HJ, Han HD, Cho MS, Rupaimoole R, Mangala LS, Sehgal V, Oh SC, Liu J, Lee JS, Coleman RL, Ram P, Lopez-Berestein G, Fidler IJ, Sood AK. Hematogenous metastasis of ovarian cancer: rethinking mode of spread. Cancer cell. 2014, 26(1): 77-91.

Prassas I, Eissa A, Poda G, Diamandis EP. Unleashing the therapeutic potential of human kallikrein-related serine proteases. Nat Rev Drug Discov. 2015, 14(3): 183-202.

Prezas P, Arlt MJ, Viktorov P, Soosaipillai A, Holzscheiter L, Schmitt M, Talieri M, Diamandis EP, Kruger A, Magdolen V. Overexpression of the human tissue kallikrein genes KLK4, 5, 6, and 7 increases the malignant phenotype of ovarian cancer cells. Biol Chem. 2006, 387(6): 807-11.

Pujade-Lauraine E, Ledermann JA, Selle F, Gebski V, Penson RT, Oza AM, Korach J, Huzarski T, Poveda A, Pignata S, Friedlander M, Colombo N, Harter P, Fujiwara K, Ray-Coquard I, Banerjee S, Liu J, Lowe ES, Bloomfield R, Pautier P. Olaparib tablets as maintenance therapy in patients with platinum-sensitive, relapsed ovarian cancer and a BRCA1/2 mutation (SOLO2/ENGOT-Ov21): a double-blind, randomised, placebo-controlled, phase 3 trial. The Lancet Oncology. 2017, 18(9): 1274-84.

Rose AM, Krishan A, Chakarova CF, Moya L, Chambers SK, Hollands M, Illingworth JC, Williams SMG, McCabe HE, Shah AZ, Palmer CNA, Chakravarti A, Berg JN, Batra J, Bhattacharya SS. MSR1 repeats modulate gene expression and affect risk of breast and prostate cancer. Ann Oncol. 2018, 29(5): 1292-303.

Rottenberg S, Jaspers JE, Kersbergen A, van der Burg E, Nygren AOH, Zander SAL, Derksen PWB, de Bruin M, Zevenhoven J, Lau A, Boulter R, Cranston A, O'Connor MJ, Martin NMB, Borst P, Jonkers J. High sensitivity of BRCA1-deficient mammary tumors to the PARP inhibitor AZD2281 alone and in combination with platinum drugs. Proc Natl Acad Sci USA. 2008, 105(44): 17079-84.

Sabatucci I, Maltese G, Lepori S, Tripodi E, Bogani G, Lorusso D. Rucaparib: a new treatment option for ovarian cancer. Expert Opin Pharmacother. 2018, 19(7): 765-71.

Salgado R, Denkert C, Demaria S, Sirtaine N, Klauschen F, Pruneri G, Wienert S, Van den Eynden G, Baehner FL, Penault-Llorca F, Perez EA, Thompson EA, Symmans WF, Richardson AL, Brock J, Criscitiello C, Bailey H, Ignatiadis M, Floris G, Sparano J, Kos Z, Nielsen T, Rimm DL, Allison KH, Reis JS, Loibl S, Sotiriou C, Viale G, Badve S, Adams S, Willard-Gallo K, Loi S. The evaluation of tumor-infiltrating lymphocytes (TILs) in breast cancer: recommendations by an International TILs Working Group 2014. Ann Oncol. 2015, 26(2): 259-71.

Sano A, Sangai T, Maeda H, Nakamura M, Hasebe T, Ochiai A. Kallikrein 11 expressed in human breast cancer cells releases insulin-like growth factor through degradation of IGFBP-3. Int J Oncol. 2007, 30(6): 1493-8.

Schmitt M, Magdolen V, Yang F, Kiechle M, Bayani J, Yousef GM, Scorilas A, Diamandis EP, Dorn J. Emerging clinical importance of the cancer biomarkers kallikrein-related peptidases (KLK) in female and male reproductive organ malignancies. Radiol Oncol. 2013, 47(4): 319-29.

Sharma M, Chuang WW, Sun Z. Phosphatidylinositol 3-kinase/Akt stimulates androgen pathway through GSK3beta inhibition and nuclear beta-catenin accumulation. J Biol Chem. 2002, 277(34): 30935-41.

Shaw JL, Diamandis EP. Regulation of human tissue kallikrein-related peptidase expression by steroid hormones in 32 cell lines. Biol Chem. 2008, 389(11): 1409-19.

Shaw JL, Grass L, Sotiropoulou G, Diamandis EP. Development of an immunofluorometric assay for human kallikrein 15 (KLK15) and identification of KLK15 in tissues and biological fluids. Clin Biochem. 2007, 40(1-2): 104-10.

Sheng L, Anderson PH, Turner AG, Pishas KI, Dhatrak DJ, Gill PG, Morris HA, Callen DF. Identification of vitamin D3 target genes in human breast cancer tissue. J Steroid Biochem Mol Biol. 2016, 164: 90-7.

Shigemasa K, Gu L, Tanimoto H, O'Brien TJ, Ohama K. Human kallikrein gene 11 (KLK11) mRNA overexpression is associated with poor prognosis in patients with epithelial ovarian cancer. Clin Cancer Res. 2004, 10(8): 2766-70.

Skacel M, Skilton B, Pettay JD, Tubbs RR. Tissue microarrays: A powerful tool for high-throughput analysis of clinical specimens - a review of the method with validation data. Appl Immunohistochem Mol Morphol. 2002, 10(1): 1-6.

Sidiropoulos KG, Ding Q, Pampalakis G, White NM, Boulos P, Sotiropoulou G, Yousef GM. KLK6-regulated miRNA networks activate oncogenic pathways in breast cancer subtypes. Mol Oncol. 2016, 10(7): 993-1007.

Soong TR, Howitt BE, Miron A, Horowitz NS, Campbell F, Feltmate CM, Muto MG, Berkowitz RS, Nucci MR, Xian W, Crum CP. Evidence for lineage continuity between early serous proliferations (ESPs) in the Fallopian tube and disseminated high-grade

serous carcinomas. J Pathol. 2018, 246(3): 344-351.

Sotiropoulou G, Pampalakis G, Diamandis EP. Functional roles of human kallikrein-related peptidases. J Biol Chem. 2009, 284(48): 32989-94.

Stephan C, Yousef GM, Scorilas A, Jung K, Jung M, Kristiansen G, Hauptmann S, Bharaj BS, Nakamura T, Loening SA, Diamandis EP. Quantitative analysis of kallikrein 15 gene expression in prostate tissue. J Urol. 2003, 169(1): 361-4.

Strickland KC, Howitt BE, Shukla SA, Rodig S, Ritterhouse LL, Liu JF, Garber JE, Chowdhury D, Wu CJ, D'Andrea AD, Matulonis UA, Konstantinopoulos PA. Association and prognostic significance of BRCA1/2-mutation status with neoantigen load, number of tumor-infiltrating lymphocytes and expression of PD-1/PD-L1 in high grade serous ovarian cancer. Oncotarget. 2016, 7(12): 13587-98.

Tamir A, Jag U, Sarojini S, Schindewolf C, Tanaka T, Gharbaran R, Patel H, Sood A, Hu W, Patwa R, Blake P, Chirina P, Oh Jeong J, Lim H, Goy A, Pecora A, Suh KS. Kallikrein family proteases KLK6 and KLK7 are potential early detection and diagnostic biomarkers for serous and papillary serous ovarian cancer subtypes. J Ovarian Res. 2014, 7: 109.

Torre LA, Bray F, Siegel RL, Ferlay J, Lortet-Tieulent J, Jemal A. Global cancer statistics, 2012. CA Cancer J Clin. 2015, 65(2): 87-108.

Torre LA, Trabert B, DeSantis CE, Miller KD, Samimi G, Runowicz CD, Gaudet MM, Jemal A, Siegel RL. Ovarian cancer statistics, 2018. CA Cancer J Clin. 2018, 68(4): 284-96.

Tothill RW, Tinker AV, George J, Brown R, Fox SB, Lade S, Johnson DS, Trivett MK, Etemadmoghadam D, Locandro B, Traficante N, Fereday S, Hung JA, Chiew YE,

Haviv I, Gertig D, DeFazio A, Bowtell DD. Novel molecular subtypes of serous and endometrioid ovarian cancer linked to clinical outcome. Clin Cancer Res. 2008, 14(16): 5198-208.

Unal D, Eroglu C, Tasdemir A, Karaman H, Kurtul N, Oguz A, Goksu SS, Kaplan B. Is human kallikrein 11 in non-small cell lung cancer treated chemoradiotherapy associated with survival? Cancer Res Treat. 2016, 48(1): 98-105.

Unal D, Tasdemir A, Oguz A, Eroglu C, Cihan YB, Turak EE, Karaman H, Soyuer S. Is human kallikrein-11 in gastric cancer treated with surgery and adjuvant chemoradiotherapy associated with survival? Pathol, Research Prac. 2013, 209(12): 779-83.

Varghese F, Bukhari AB, Malhotra R, De A. IHC Profiler: an open source plugin for the quantitative evaluation and automated scoring of immunohistochemistry images of human tissue samples. PloS One. 2014, 9(5): e96801.

Wan WH, Fortuna MB, Furmanski P. A rapid and efficient method for testing immunohistochemical reactivity of monoclonal-antibodies against multiple tissue samples simultaneously. J Immunol Methods. 1987, 103(1): 121-9.

Wang Z, Ruan B, Jin Y, Zhang Y, Li J, Zhu L, Xu W, Feng L, Jin H, Wang X. Identification of KLK10 as a therapeutic target to reverse trastuzumab resistance in breast cancer. Oncotarget. 2016, 7(48): 79494-502.

Wen YG, Wang Q, Zhou CZ, Yan DW, Qiu GQ, Yang C, Tang HM, Peng ZH. Identification and validation of kallikrein-ralated peptidase 11 as a novel prognostic marker of gastric cancer based on immunohistochemistry. J Surg Oncol. 2011, 104(5): 516-24.

Wentzensen N, Poole EM, Trabert B, White E, Arslan AA, Patel AV, Setiawan VW, Visvanathan K, Weiderpass E, Adami HO, Black A, Bernstein L, Brinton LA, Buring J, Butler LM, Chamosa S, Clendenen TV, Dossus L, Fortner R, Gapstur SM, Gaudet MM, Gram IT, Hartge P, Hoffman-Bolton J, Idahl A, Jones M, Kaaks R, Kirsh V, Koh WP, Lacey JV, Lee IM, Lundin E, Merritt MA, Onland-Moret NC, Peters U, Poynter JN, Rinaldi S, Robien K, Rohan T, Sandler DP, Schairer C, Schouten LJ, Sjoholm LK, Sieri S, Swerdlow A, Tjonneland A, Travis R, Trichopoulou A, van den Brandt PA, Wilkens L, Wolk A, Yang HP, Zeleniuch-Jacquotte A, Tworoger SS. Ovarian cancer risk factors by histologic subtype: an analysis from the ovarian cancer cohort consortium. J Clin Oncol. 2016, 34(24): 2888-98.

Werle E. On the kallikrein in blood. Biochemische Zeitschrift. 1936, 287(3/4): 235-61.

Wiegand KC, Shah SP, Al-Agha OM, Zhao Y, Tse K, Zeng T, Senz J, McConechy MK, Anglesio MS, Kalloger SE, Yang W, Heravi-Moussavi A, Giuliany R, Chow C, Fee J, Zayed A, Prentice L, Melnyk N, Turashvili G, Delaney AD, Madore J, Yip S, McPherson AW, Ha G, Bell L, Fereday S, Tam A, Galletta L, Tonin PN, Provencher D, Miller D, Jones SJ, Moore RA, Morin GB, Oloumi A, Boyd N, Aparicio SA, Shih Ie M, Mes-Masson AM, Bowtell DD, Hirst M, Gilks B, Marra MA, Huntsman DG. ARID1A mutations in endometriosis-associated ovarian carcinomas. New Engl J Med. 2010, 363(16): 1532-43.

Xu B, Lefringhouse J, Liu Z, West D, Baldwin LA, Ou C, Chen L, Napier D, Chaiswing L, Brewer LD, St Clair D, Thibault O, van Nagell JR, Zhou BP, Drapkin R, Huang JA, Lu ML, Ueland FR, Yang XH. Inhibition of the integrin/FAK signaling axis and c-Myc synergistically disrupts ovarian cancer malignancy. Oncogenesis. 2017, 30(6): e295.

Xu CH, Zhang Y, Yu LK. The diagnostic and prognostic value of serum human kallikrein-related peptidases 11 in non-small cell lung cancer. Tumour Biol. 2014, 35(6): 5199-203.

Yang F, Aubele M, Walch A, Gross E, Napieralski R, Zhao S, Ahmed N, Kiechle M, Reuning U, Dorn J, Sweep F, Magdolen V, Schmitt M. Tissue kallikrein-related peptidase 4 (KLK4), a novel biomarker in triple-negative breast cancer. Biol Chem. 2017, 398(10): 1151-64.

Yang F, Hu ZD, Chen Y, Hu CJ. Diagnostic value of KLK6 as an ovarian cancer biomarker: a meta-analysis. Biomed Rep. 2016, 4(6): 681-6.

Yang F, Li JY, Yin QN, Yang K, Dong SN, Bai LJ, Liu P, Tong XW. Human kallikrein 5 as a novel prognostic biomarker for triple-negative breast cancer: tissue expression analysis and relationship with disease course. Genet Mol Res. 2015, 14(3): 9655-66.

Yoon H, Blaber SI, Debela M, Goettig P, Scarisbrick IA, Blaber M. A completed KLK activome profile: investigation of activation profiles of KLK9, 10, and 15. Biol Chem. 2009, 390(4): 373-7.

Yoon H, Blaber SI, Evans DM, Trim J, Juliano MA, Scarisbrick IA, Blaber M. Activation profiles of human kallikrein-related peptidases by proteases of the thrombostasis axis. Protein Sci. 2008, 17(11): 1998-2007.

Yoon H, Blaber SI, Li W, Scarisbrick IA, Blaber M. Activation profiles of human kallikrein-related peptidases by matrix metalloproteinases. Biol Chem. 2013, 394(1): 137-47.

Yoon H, Laxmikanthan G, Lee J, Blaber SI, Rodriguez A, Kogot JM, Scarisbrick IA, Blaber M. Activation profiles and regulatory cascades of the human kallikrein-related peptidases. J Biol Chem. 2007, 282(44): 31852-64.

Yousef GM, Chang A, Scorilas A, Diamandis EP. Genomic organization of the human kallikrein gene family on chromosome 19q13.3-q13.4. Biochem Biophys Res Commun.

2000, 276(1): 125-33.

Yousef GM, Diamandis EP. The new human tissue kallikrein gene family: structure, function, and association to disease. Endocr Rev. 2001, 22(2): 184-204.

Yousef GM, Polymeris ME, Yacoub GM, Scorilas A, Soosaipillai A, Popalis C, Fracchioli S, Katsaros D, Diamandis EP. Parallel overexpression of seven kallikrein genes in ovarian cancer. Cancer Res. 2003, 63(9): 2223-7.

Yousef GM, Scorilas A, Jung K, Ashworth LK, Diamandis EP. Molecular cloning of the human kallikrein 15 gene (KLK15). Up-regulation in prostate cancer. J Biol Chem. 2001, 276(1): 53-61.

Yousef GM, Scorilas A, Katsaros D, Fracchioli S, Iskander L, Borgoño C, Rigault de la Longrais IA, Puopolo M, Massobrio M, Diamandis EP. Prognostic value of the human kallikrein gene 15 expression in ovarian cancer. J Clin Oncol. 2003, 21(16): 3119-26.

Yousef GM, Scorilas A, Magklara A, Memari N, Ponzone R, Sismondi P, Biglia N, Abd Ellatif M, Diamandis EP. The androgen-regulated gene human kallikrein 15 (KLK15) is an independent and favourable prognostic marker for breast cancer. Br J Cancer. 2002, 87(11): 1294-300.

10. List of publications

1. Geng X, Liu Y, Diersch S, Kotzsch M, Grill S, Weichert W, Kiechle M, Magdolen V, Dorn J. Clinical relevance of kallikrein-related peptidase 9, 10, 11, and 15 mRNA expression in advanced high-grade serous ovarian cancer. PLoS One, 2017, 12(11): e0186847.

2. Geng X, Liu Y, Dreyer T, Bronger H, Drecoll E, Magdolen V, Dorn J. Elevated tumor tissue protein expression levels of kallikrein-related peptidases KLK10 and KLK11 are associated with a better prognosis in advanced high-grade serous ovarian cancer patients. Am J Cancer Res, 2018, 8(9): 1856-64.

3. Geng X, Liu Y, Diersch S, Kotzsch M, Weichert W, Kiechle M, Magdolen V, Dorn J. Clinical relevance of kallikrein-related peptidase 9, 10, 11, and 15 mRNA expression in advanced high-grade serous ovarian cancer. 34th winter school on proteases and inhibitors. 2017, Mar 8-12th, Tiers, Italy. Oral presentation.

4. Geng X, Liu Y, Dreyer T, Seidl C, Kiechle M, Dorn J, Magdolen V, Drecoll E. Establishment of immunohistochemistry for kallikrein-related peptidase 10 (KLK10) and 11 (KLK11) protein expression in high-grade advanced (FIGOIII/IV) serous ovarian cancer. 7th Symposium on kallikreins and kallikrein-related peptidases (ISK2017). 2017, Sep 26-29th, Tours, France. Poster and oral presentation.

5. Geng X, Liu Y, Dreyer T, Seidl C, Kiechle M, Magdolen V, Dorn J, Drecoll E. Tumor tissue protein expression levels of kallikrein-related peptidase (KLK) 10 and 11 are associated with prognosis of advanced high-grade serous ovarian cancer patients. 35th winter school on proteases and inhibitors. 2018, Feb 28th–Mar 4th, Tiers, Italy. Oral presentation.

11. Acknowledgements

First of all, I owe this sincere gratitude to my study-coach Prof. Dr. rer. nat. Viktor Magdolen, many thanks for providing me the opportunity to explore a period of my life in Munich. He put in much patience and energy through my study being truly caring and supportive. My sincere appreciation goes to Dr. MD Julia Dorn, for her warmly helpful guidance in group work, to Dr. Eva Groß for her kind took-over as my mentor, to Prof. Dr. rer. nat. Ute Reuning for her meaningful teaching in seminars. In addition, I would like to show my respect and gratitude to Prof. Dr. rer. nat. Manfred Schmitt, he actually started my opportunity in this group.

Very special gratitude to dear Sandra Diersh, she is a wonderful supervisor helping me in every problem, I will miss the working days spending with her. I am very grateful to my co-workers who have contributed to this project, to Yueyang Liu for his long-time and important cooperation during this work, to Tobias Dreyer for his very supportive work in every aspects, to Christof Seidl for his thoughtful and kindly work to correct my thesis, to Nancy Ahmed, Larissa Dettmar and Sarah Pries for their previously established work of this project. Moreover, I am very grateful to the university faculty members who joined my paper writing, to Holger Bronger, Marion Kiechle, Matthias Kotzsch, Sabine Grill, and Wilko Weichert, for their nice suggestion and revised working during paper publication.

I am very thankful to dear colleague staff in our lab, they taught me a lot during my study. To Enken Drecoll, she guided me in the immunohistochemistry experiments. To Daniela Hellmann, her enthusiasm encouraged me in regular work. To Sabine Creutzburg, I admired and learned from her in her elegant working. To Elisabeth Schueren, I will remember her diligent and helpful working early in the morning. To Anke Benge, she helped a lot in daily lab time. To Natalie Falkenberg, she gave nice proposals for my seminar presentation. To Rudolf Napieralski, although short working time together, we had interesting chats. Importantly, I am very grateful to dear friends

I met here, to Shuo Zhao, Weiwei Gong, Ping Wang, Christoph Stange, Johanna Felber. It is a great pleasure to share working time with all of you, thanks a lot for being so helpful and warm either for work or life. Finally, but not to least, I owe heartfelt gratitude to my eternal supporters, my parents, their love and company encourage me to face everything.

Many thanks to all!